Experimental and Computational Spectroscopic Studies of the Isomers and Conformations of Dibenzylideneacetone

By

Zachary B. Richardson

A Major Qualifying Project

Submitted to the Faculty

Of the

Worcester Polytechnic Institute

In partial fulfillment of the requirements for the

Degree of Bachelor of Science

In

Chemistry

APPROVED:

_____

ABSTRACT

This project examines the conformational isomers of dibenzylideneacetone through infrared and UV-vis absorption spectra as well as quantum molecular modeling. Experiments followed the procedures of previously published experiments of dibenzylideneacetone, in hopes of interpreting the results.

ACKNOWLEDGEMENTS

Thanks to Professor Connors for taking me into this project and not giving up on me. Thanks to Dr. Christopher Zoto for helping me along the way, Worcester Polytechnic institute for four amazing years and change and my ~~girlfriend~~ fiancée Sarah-Beth for being the greatest person on earth the last two years and four months.

Contents

List of figures

List of Tables

Introduction

Dibenzylideneacetone, here for known as DBZA is a ketone whose formula is $C_{17}H_{14}O$. DBZA is a flaky, low density yellow solid at room temperature and only dissolves in a small number of solvents. The physical properties of DBZA are as shown as compared to benzaldehyde and acetone:

Material	Benzaldehyde	Acetone	(E,E)- Dibenzylideneacetone
Molecular weight **[g/mol]**	106.12	58.08	234.30
Density [g/ml]	1.05	0.79	-
Melting point [°C]			107 –
n [mmol]	47.2	23.0	12.1
Mass [g]	5.01	1.34	10.45
Volume [ml]	4.77	1.70	-
Neq	2	1	-
Company	Acros Organics	Fluka	-
Purity	> 98%	> 99.7%	-
Risk and Safety **Statements**	R 22 S 24	R 11-36-66-67- 39/23/24/25-	S 22-24/25

Table 1: DBZA Physical properties compared to its components. (Vaucher 2010)

DBZA is formed from an aldol condensation where benzaldehyde (2 mole eq.) and acetone (1 mole eq.) in sodium hydroxide base and an ethanol solvent (Vaucher). DBZA is used as a sun screening agent due to sunlight eventually isomerizing the ketone into cyclobutanes (Huck and Leigh). DBZA is also used extensively in inorganic chemistry as a ligand for Palladium (0) as well as Platinum (0), both very rare and unreactive metals. Tris (Dibenzylideneacetone)

dipalladium has been proven effective against melanoma growth (Bhandarkar et al). This compound's uses have warranted further study of its properties.

Experimental

DBZA is a compound with two rotational degrees of freedom, thus DBZA exhibits three conformational isomers under various conditions (Venkateshwarlu and Subrahmanyam). These three rotational isomers, cis-cis (here forth referred to as EE), cis-trans (here forth referred to as ZE), and trans-trans (here forth referred to as ZZ) differ at the second and fourth carbons on the central 1,5-dibenzylpentadi-2,4-ene-3-one chain. Tanaka et al hypothesized the bond angles and lengths for all three isomers based on standard bond length knowledge for C=O, C-H and C=C bonds in unsaturated compounds. At first the EE was believed to be the dominant form (Tanaka et al), and its structure can be seen here from ChemDraw.

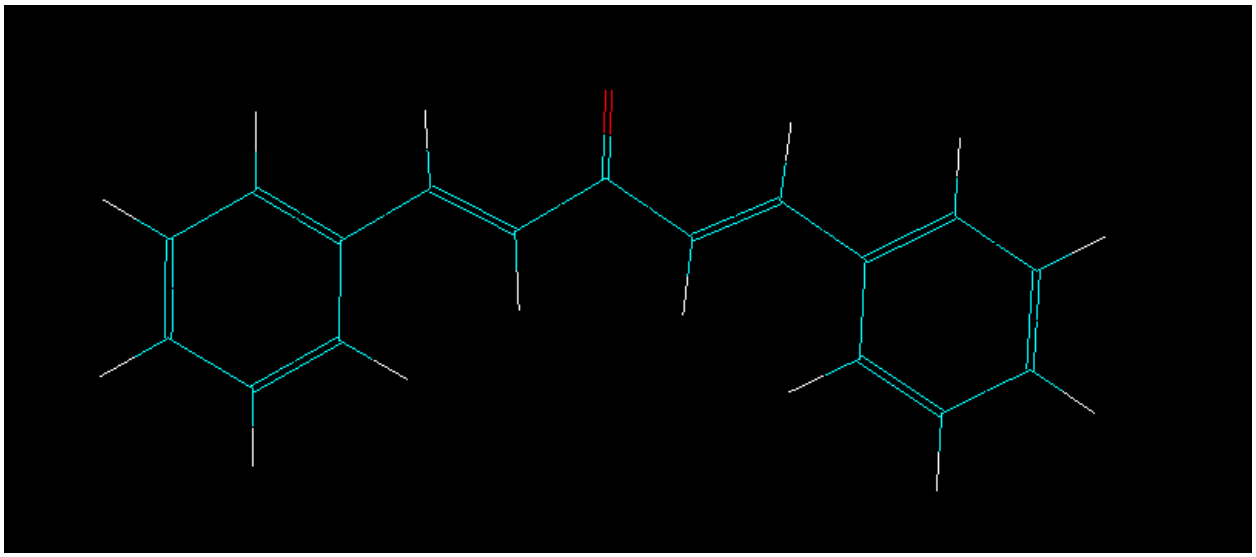

Figure 1: ChemDraw structure of the major conformer of DBZA

This hypothesis stemmed from room temperature Kerr values studies and visible polarization values in order to determine the main conformer in solid DBZA (Bramley and Le

Fèvre). Also, these conformers have widely varying energies of formation, as noted by Tanaka, et al in their nuclear magnetic resonance study of the compound at room temperature:

INDO total energies ΔE_t, electronic energies ΔE_e, and core repulsion energies ΔE_c of the three planar conformations of DBA (in eV)

Conformation	ΔE_e	ΔE_c	ΔE_t
s-*cis*,*cis*	0.000	0.000	0.000
s-*cis*,*trans*	−224.947	225.075	0.128
s-*trans*,*trans*	−749.426	757.436	8.010

The energies of the s-*cis*,*cis* form are taken as the base: E_e −18 445.862, E_c 14 518.070, E_t −3 927.792 eV.

Table 2: ΔE values from room temperature NMR study (Tanaka et al 1978)

Here, through NMR spectroscopy, Tanaka et al concluded that evidence was found for the room temperature presence of just two planar conformers, a major (EE) and a minor (ZE), due to the disproportionately high ΔE for a (ZZ) planar conformer. This finding relates strongly to an older infrared spectrum study, where a two conformer hypothesis was supported by a claim of two C=O region bands for DBZA in carbon tetrachloride, and the authors used dipole moments to support their hypothesis, rather than test for bond angles or electronic transitions (Tsukerman et al 1968). These studies inspired an ultraviolet spectrum study of DBZA, first at room temperature, and then at 101 K, only to discover that form ZE is actually non-planar at room temperature or higher, with a torsion angle that increases with an increase in the first $\pi^* \leftarrow \pi$ shift of location, given that in ketones this shift has the lowest energy (Hoshi et al 1986). Their UV visible spectrum in n-hexane is shown here.

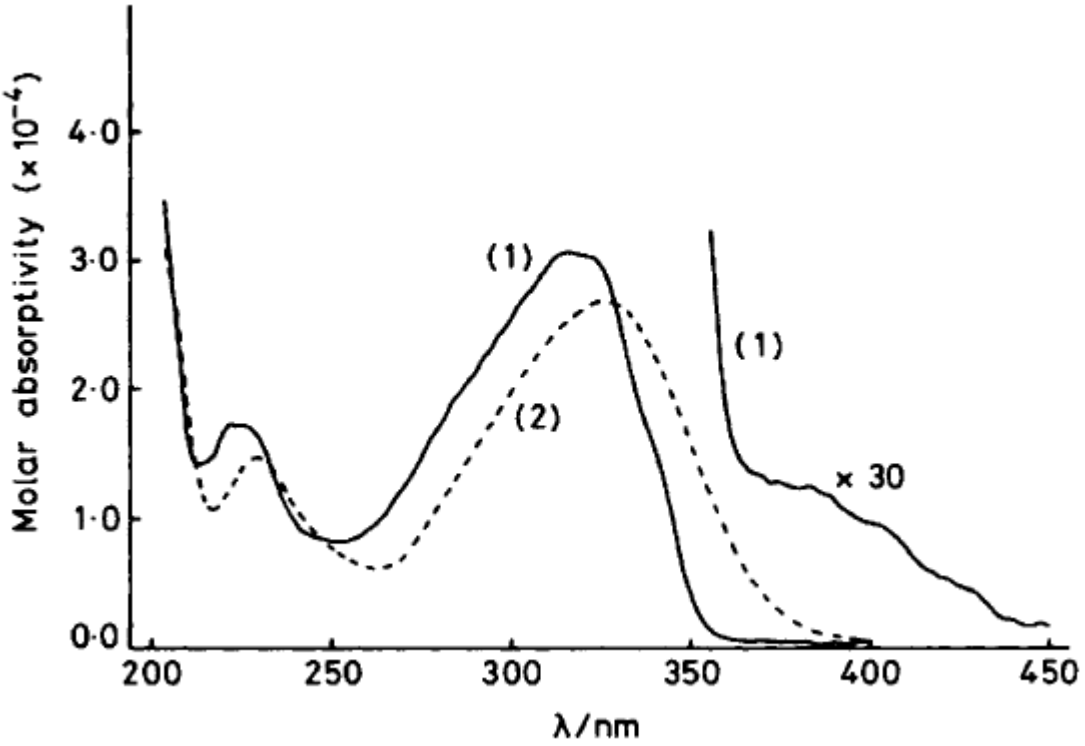

Figure 2: UV Visible spectrum of concentrated and 30X diluted SBZA in n-hexane (Hoshi et al)

Armed with this knowledge, Venkateshwarlu and Subrahmanyam studied the infrared spectra of DBZA in carbon tetrachloride, chloroform and dichloromethane solvents, to discover evidence for three hypothesized conformers, EE, ZE, and a non-planar ZZ isomer. Venkateshwarlu's and Subrahmanyam's hypothesis would be tested based on carbon-oxygen double bond frequencies observed in the IR spectrum, and how well their peaks confirm to known carbon-oxygen double bond frequencies from their researched table:

Conformer	CCl_4 frequency cm^{-1} And relative intensity	$CHCl_3$ frequency cm^{-1} And relative intensity	CH_2Cl_2 frequency cm^{-1} And relative intensity
C=O Cis-Cis	1676 (0.2107)	1671 (0.1750)	1674 (0.1644)
C=O Cis-Trans	1655 (0.4676)	1653 (0.4270)	1654 (0.3920)
C=O Trans-Trans	1650 (0.3216)	1648 (0.3970)	1649 (0.4430)

Table 3: Determined C=O stretching frequencies of DBZA (Venkateshwarlu and Subrahmanyam)

They came to observe a triplet peak all three times in the C=O regions they had hypothesized, as seen here:

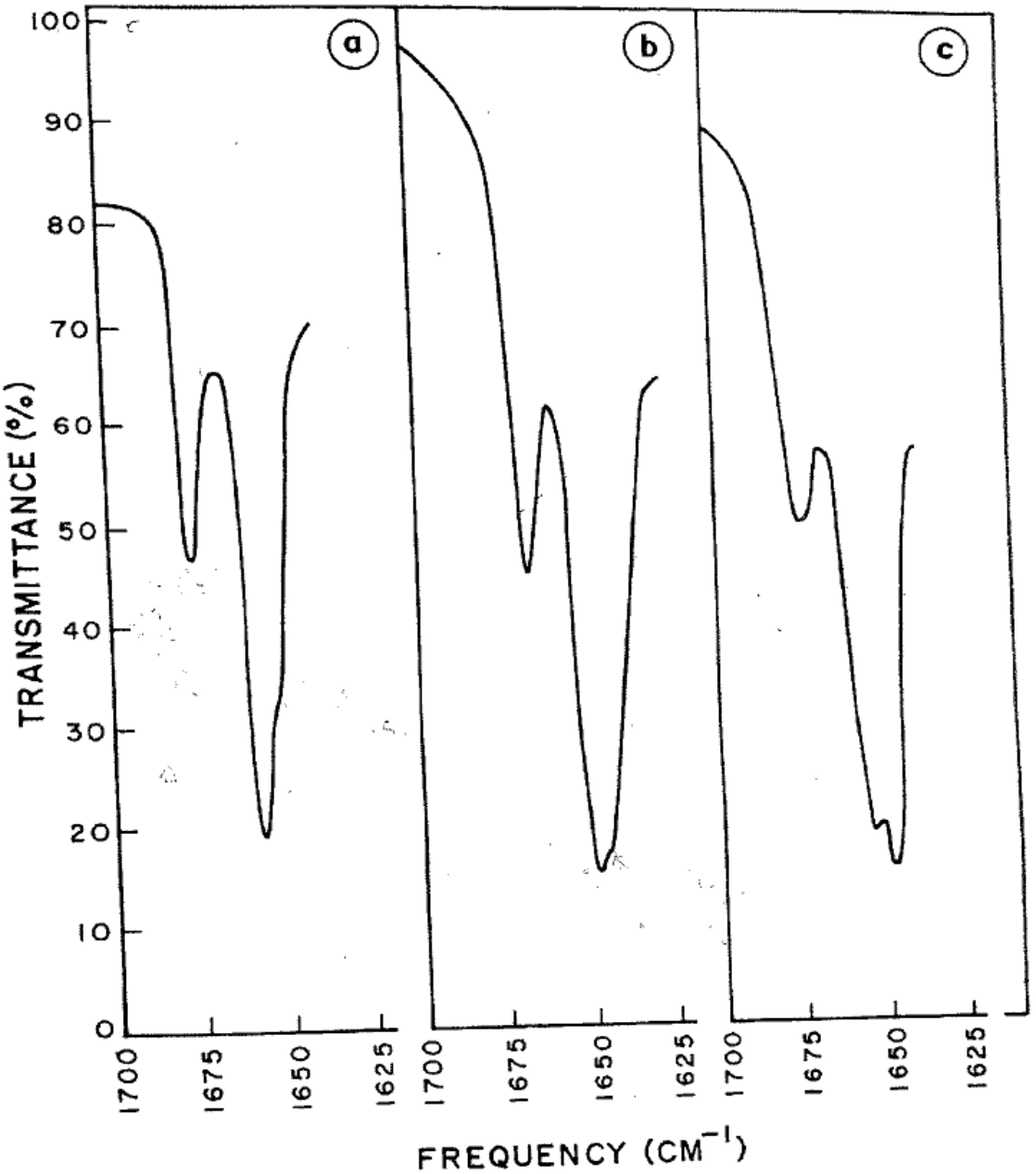

Figure 3. The C=O bands of DBA in different solvents. (a) CCl_4. (b) $CHCl_3$. (c) CH_2Cl_2.

Figure 3: Venkateshwarlu and Subrahmanyam IR results in CCl_4, $CHCl_3$ and CH_2Cl_2

This peak from (1655 to 1645 cm^{-1}) is a doublet whose right side intensity increased with more polar solvents, with dichloromethane being the most pronouncedly so, decreasing to chloroform and carbon tetrachloride (Venkateshwarlu and Subrahmanyam). This side of the triplet was concluded to confirm to the ZZ isomer, increased in intensity and therefore frequency with more polar solvents (Venkateshwarlu and Subrahmanyam). This strain created a skewed conformer, which is the only possible setup for the ZZ isomer they hypothesized. The increased presence of ZE and EE conformers in less polar solvents was hypothesized to be the result of steric hindrance from polar solvents of non-skewed conformers.

This skewed conformation is the result of strong π electron repulsion and the high polarity displayed by the ZZ DBZA conformer (Venkateshwarlu and Subrahmanyam 1987). The following experiments seek to confirm the findings by Venkateshwarlu and Subrahmanyam using two infrared spectra devices and the same three solvents, as well as quantum chemical modeling. The absorption spectra data will be tested for as well to confirm the Hoshi et al results. Quantum chemical modeling will be used to observe the optimized shapes and structural data of each isomer.

Structural Data

Through thorough quantum chemical modeling studies, the structures of all three conformers of DBZA were calculated at the DFT B3LYP/6-311+G(d,p) level of theory. The 6-311+G(d,p) level of theory is the largest basis set of DFT and the most accurate of the set of basis sets. The optimized forms of the conformers below were generated:

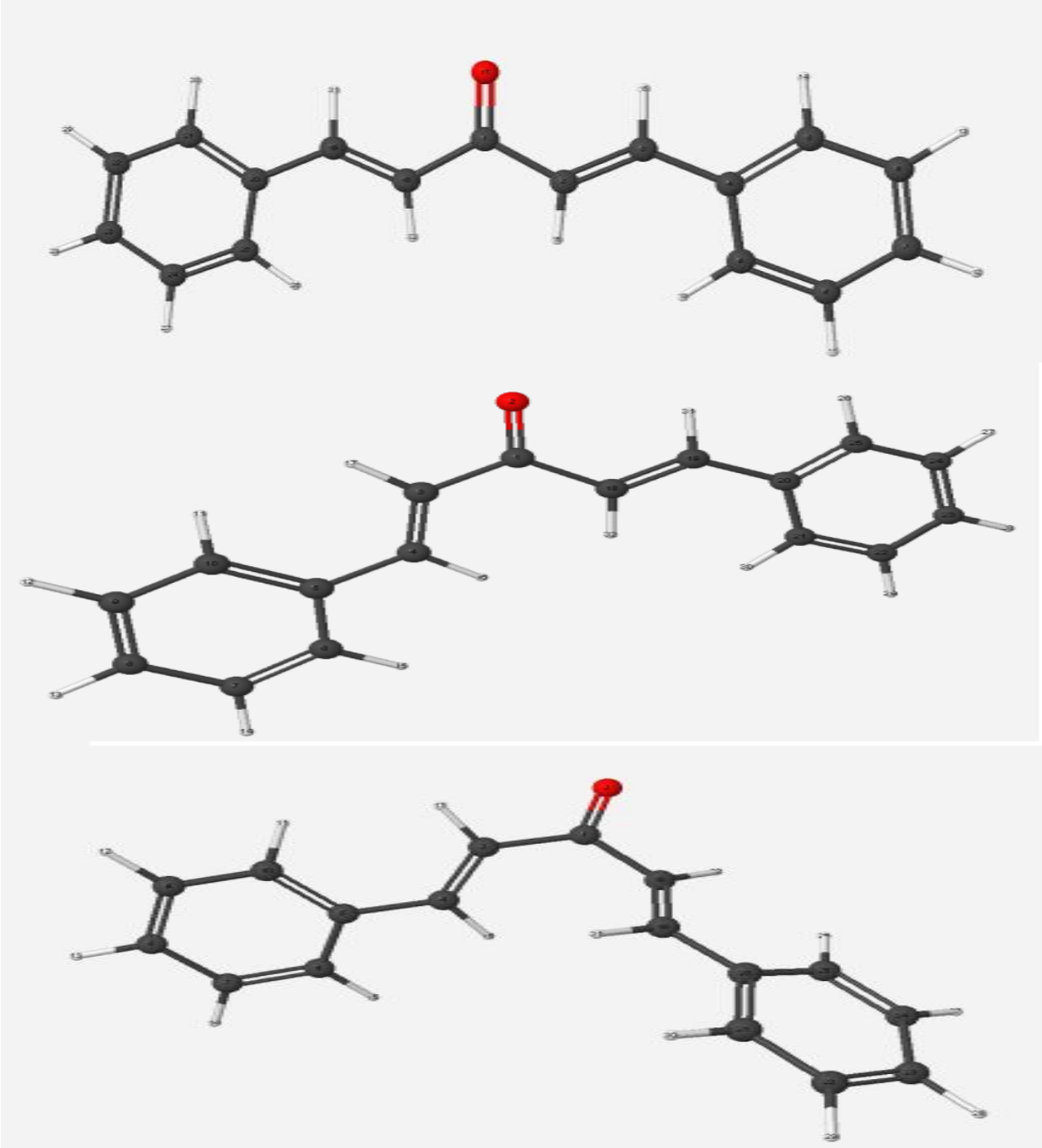

Figure 4: WebMO generated optimized forms of EE, ZE and ZZ Conformers

The skewed ZZ conformation obtained by Venkateshwarlu and Subrahmanyam became a reality, as a high bond angle between the first three carbons of the central 2,4-pentadiene-3-one chain was required to create a non-resonating and stable ZZ conformer.

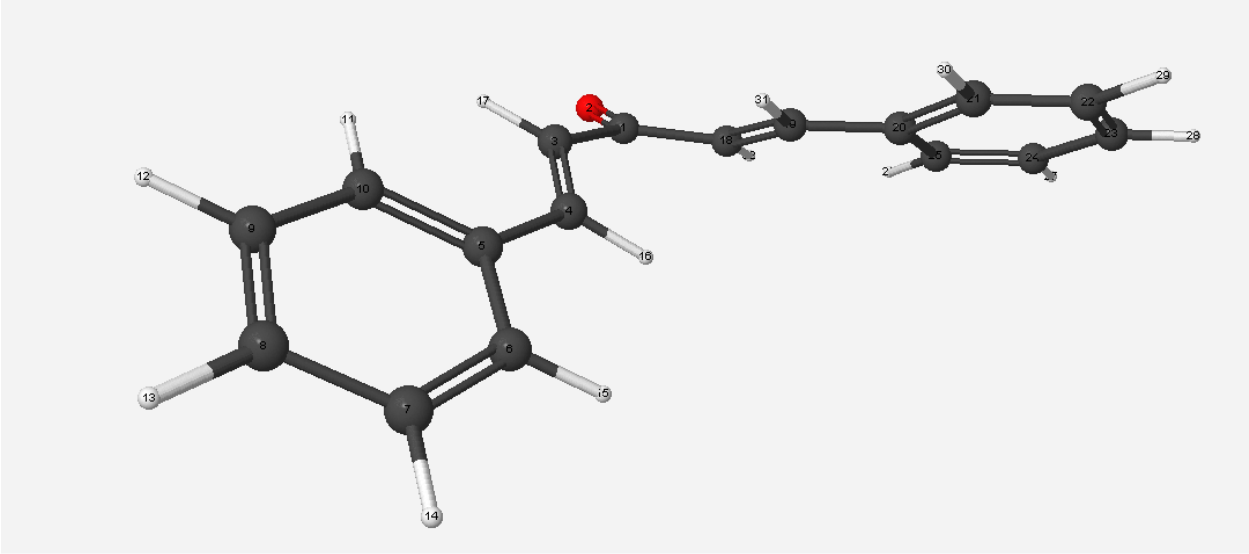

Figure 5: ZZ conformer skew side view

Bond lengths and angles have also been determined at the DFT B3LYP/6-311+G(d,p) level of theory. The following bond lengths were obtained from the optimized EE conformer in air.

Bond Number	Region	Bond Length (Å)
R1	R(1,2) C-C	1.4843
R2	R(1,17) C=O	1.2265
R3	R(1,18)C-C	1.4843
R4	R(2,3) C=C	1.3452
R5	R(2,16) C-H	1.0852
R6	R(3,4) C-C	1.4614
R7	R(3,15) C-H	1.0878
R8	R(4,5) C-C	1.4053
R9	R(4,9) C=C	1.407
R10	R(5,6) C=C	1.3917
R12	R(6,7) C-C	1.393
R14	R(7,8) C=C	1.3973
R16	R(8,9) C-C	1.3883
R19	R(18,19) C=C	1.3452
R21	R(19,20) C-C	1.4614
R23	R(20,21) C=C	1.4053
R24	R(20,25) C-C	1.407
R25	R(21,22) C-C	1.3917
R27	R(22,23) C=C	1.393
R29	R(23,24) C-C	1.3973
R31	R(24,25) C=C	1.3883

Table 4: C-C, C=O, C=C, and the center C-H bond lengths for the EE Isomer

These values largely followed the predicted ones by Tanaka et al. The exceptions being that the single bonded carbon atoms along the 2,4-pentadiene-3-one chain had bond lengths that were 4 angstroms longer than the benzene carbon-carbon single bonds, and the double bonds of the 2,4-pentadiene-3-one were .552 angstroms shorter than the benzene carbon double bonds.

Bond angles were examined next for all C=C-C and C-C=O regions of the EE conformer. These angles in an air optimized structure are as follows.

Angle	Location (All are C=C-C unless otherwise labeled)	Angle
A1	A(2,1,17) C-C=O	122.1456
A2	A(2,1,18)	115.7088
A3	A(17,1,18) O=C-C	122.1456
A4	A(1,2,3)	121.0994
A7	A(2,3,4)	128.1149
A10	A(3,4,5)	118.5621
A11	A(3,4,9)	123.3655
A12	A(5,4,9)	118.0724
A13	A(4,5,6)	121.1483
A16	A(5,6,7)	119.9796
A19	A(6,7,8)	119.653
A22	A(7,8,9)	120.3418
A25	A(4,9,8)	120.8049
A28	A(1,18,19)	121.0994
A31	A(18,19,20)	128.1149
A34	A(19,20,21)	118.5621
A35	A(19,20,25)	123.3655
A36	A(21,20,25)	118.0724
A37	A(20,21,22)	121.1483
A40	A(21,22,23)	119.9796
A43	A(22,23,24)	119.653
A46	A(23,24,25)	120.3418
A49	A(20,25,24)	120.8049

Table 5: C=C-C and C-C=O Bonding angles

Here, the angle is significantly more acute for the (2,1,18) region. This is due to the oxygen polar bonded onto carbon 1. The angles are significantly more obtuse where the angle ends at 5 or 20, the beginning of the benzene rings. The fact that these carbons at the end of the benzene rings are only bonded to carbons changes the angle between the bonds slightly as compared to the carbons bonded to hydrogen and two carbons.

A similar procedure was carried out for the ZE conformer, whose optimized bond lengths are as follows:

Bond Name	Region	Bond Length (Å)
R1	R(1,2)C=O	1.2278
R2	R(1,3) C-C	1.4806
R3	R(1,18)C-C	1.4851
R4	R(3,4)C=C	1.3456
R5	R(3,17) C-H	1.0853
R6	R(4,5)C-C	1.4654
R7	R(4,16) C-H	1.0861
R8	R(5,6) C-C	1.4049
R9	R(5,10) C=C	1.4065
R10	R(6,7) C=C	1.3917
R12	R(7,8) C-C	1.3929
R14	R(8,9) C=C	1.397
R16	R(9,10) C-C	1.3885
R19	R(18,19) C=C	1.3444
R21	R(19,20)C-C	1.4624
R23	R(20,21) C-C	1.4068
R24	R(20,25) C=C	1.4052
R25	R(21,22) C=C	1.3885
R27	R(22,23) C-C	1.3972
R29	R(23,24) C=C	1.3929
R31	R(24,25) C-C	1.3918

Table 6: C-C, C=O, C=C, and the center C-H bond lengths for the ZE Isomer

The values were practically identical to those of the EE isomer. The ZE isomer had carbon-carbon-carbon and oxygen-carbon-carbon bond angles as such:

Angle	Location (All are C=C-C unless otherwise labeled)	Angle
A1	A(2,1,3) O=C-C	118.5711
A2	A(2,1,18) O=C-C	121.486
A3	A(3,1,18) C-C=C	119.943
A4	A(1,3,4)	126.9345
A7	A(3,4,5)	127.0815
A10	A(4,5,6)	118.6523
A11	A(4,5,10)	123.2501
A12	A(6,5,10)	118.0976
A13	A(5,6,7)	121.1799
A16	A(6,7,8)	119.9493
A19	A(7,8,9)	119.6272
A22	A(8,9,10)	120.4042
A25	A(5,10,9)	120.7419
A28	A(1,18,19)	120.4792
A31	A(18,19,20)	128.0259
A34	A(19,20,21)	123.4665
A35	A(19,20,25)	118.4921
A36	A(21,20,25)	118.0414
A37	A(20,21,22)	120.8248
A40	A(21,22,23)	120.3447
A43	A(22,23,24)	119.6359
A46	A(23,24,25)	119.9791
A49	A(20,25,24)	121.1741

Table 7: C=C-C and C-C=O Bonding angles

Firstly, the oxygen-carbon-carbon region (2,1,3) had a slightly more obtuse value than the corresponding (17,1,2) region of the EE isomer. The bond angle for the (1,3,4) region is the main difference, with a more obtuse value of 127^{o}, as compared to the 121^{o} angle of the comparable (1,2,3) region of the EE conformer. This angle corresponds to the trans, or Z region of the conformer.

Finally, the skewed ZZ conformer was created and optimized at the B3LYP/6-311+G(d,p) level of theory in no solvent, after many attempts to create a sufficiently skewed conformer. The optimized bond lengths are as follows:

Bond Name	Region	Bond Length (Å)
R1	R(1,2)C=O	1.2269
R2	R(1,3) C-C	1.4832
R3	R(1,18) C-C	1.4832
R4	R(3,4) C=C	1.3449
R5	R(3,17)C-H	1.0854
R6	R(4,5) C-C	1.4665
R7	R(4,16) C-H	1.0864
R8	R(5,6) C-C	1.4047
R9	R(5,10) C=C	1.4061
R10	R(6,7) C=C	1.392
R12	R(7,8) C-C	1.3928
R14	R(8,9) C=C	1.397
R16	R(9,10) C-C	1.3887
R19	R(18,19) C=C	1.3449
R21	R(19,20) C-C	1.4665
R23	R(20,21) C=C	1.4047
R24	R(20,25) C-C	1.4061
R25	R(21,22) C-C	1.392
R27	R(22,23) C=C	1.3928
R29	R(23,24) C-C	1.397
R31	R(24,25) C=C	1.3887

Table 8: C-C, C=O, C=C, and the center C-H bond lengths for the ZZ Isomer

Here, the values once again remained consistent to the EE and ZE isomers. The angles were as follows:

Angle	Location	Angle
A1	A(2,1,3) O=C-C	118.9778
A2	A(2,1,18) O=C-C	118.9779
A3	A(3,1,18) C=C-C	122.0443
A4	A(1,3,4)	125.4568
A7	A(3,4,5)	127.1818
A10	A(4,5,6)	118.6111
A11	A(4,5,10)	123.2925
A12	A(6,5,10)	118.0962
A13	A(5,6,7)	121.1773
A16	A(6,7,8)	119.9619
A19	A(7,8,9)	119.6031
A22	A(8,9,10)	120.41
A25	A(5,10,9)	120.7514
A28	A(1,18,19)	125.4568
A31	A(18,19,20)	127.1818
A34	A(19,20,21)	118.6111
A35	A(19,20,25)	123.2924
A36	A(21,20,25)	118.0962
A37	A(20,21,22)	121.1773
A40	A(21,22,23)	119.9619
A43	A(22,23,24)	119.6031
A46	A(23,24,25)	120.41

Table 9: C=C-C and C-C=O Bonding angles

Here, regions (2,1,3) and (2,1,18) involving the carbon oxygen bond had similar values to the corresponding (2,1,3) region from the ZE isomer. Compared to the ZE (1,3,4) trans-bonded side, the corresponding (1,3,4) and (1,18,19) carbon-carbon-carbon regions had slightly more acute bond angles.

The dihedral angles had to be studied to discover the true skewed nature of the ZZ conformer. The dihedral angles of carbons (1,2,4,5) from the central 2,4-pentadiene-3-one for each conformer was 359.983^{o} for the EE, 179.992^{o} for the ZE and 310.277^{o} for the ZZ. While the EE and ZE conformers' dihedral angles had radian values of roughly 2π and π, the ZZ conformer had a $7\pi/4$ radian value for its dihedral angle. The ZZ isomer had a radian value of roughly

$31\pi/18$, far from an integer value multiplied by π. Whereas the sine values of the EE and ZE dihedral angles were roughly 0, the sine value of the ZZ dihedral angle was -0.766. Subtracting the dihedral angle from 360^{o} obtained from placing the non skewed side of the ZZ conformer along the x axis, there is a 50^{o} angle between the first and last carbons of the 2,4-pentadiene-3-ol chain.

IR Spectra

In order to confirm the existence of all three conformers and the findings of Venkateshwarlu and Subrahmanyam, their experiments had to be replicated. Solid DBZA was recrystallized from ethanol and dissolved in carbon tetrachloride, chloroform and dichloromethane. Two Perkin-Elmer Spectrum One FTIR Spectrometers were used to examine these mixtures.

Dichloromethane is the most polar solvent used in this experiment; so first, IR spectra had to be taken of just the solvent, to distinguish it from the eventual addition of DBZA. The spectrum changed drastically in the carbonyl region with an addition of DBZA using the same machine. This spectrum can be seen here, zoomed into the carbonyl region (1700 to 1475 cm^{-1}).

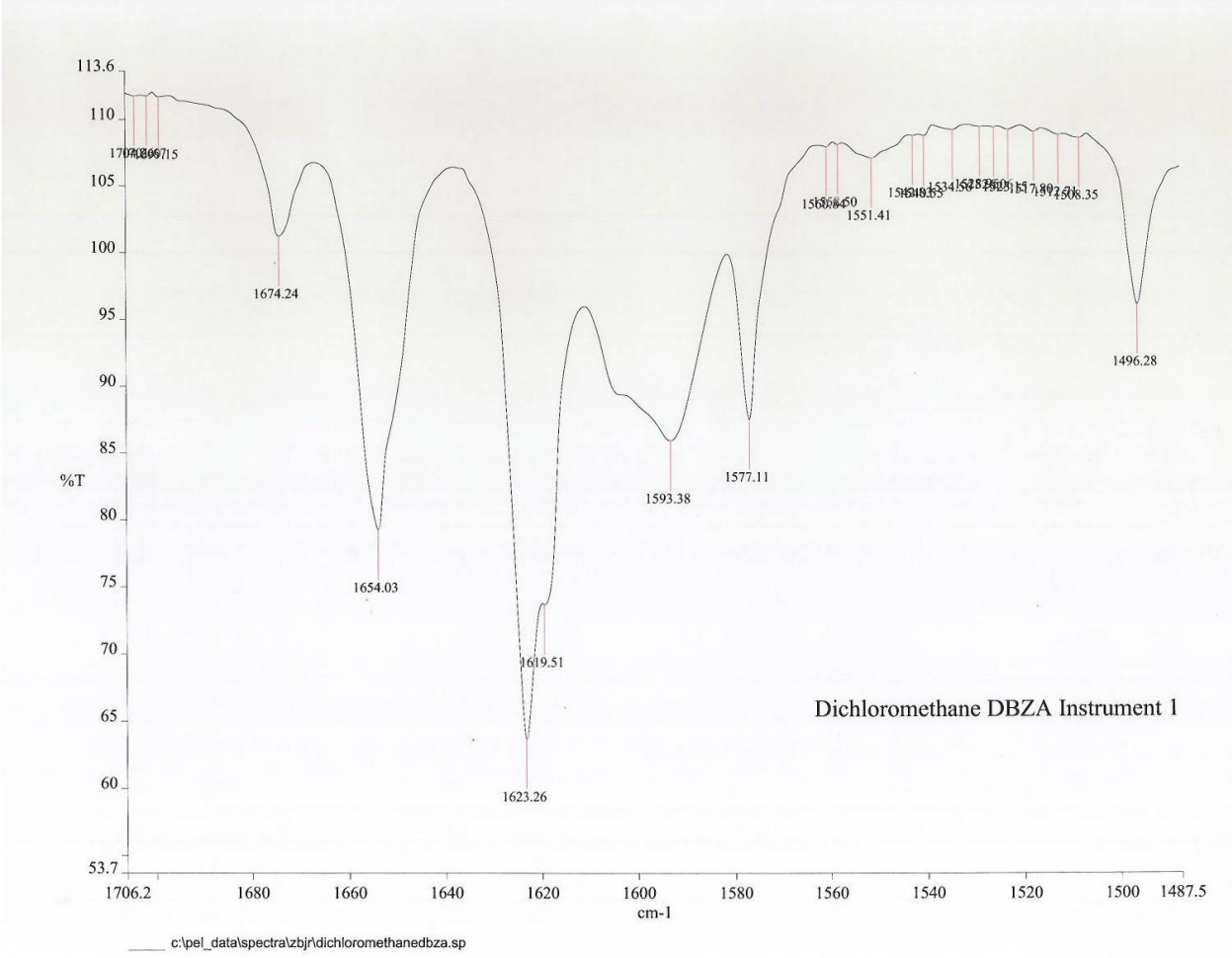

Figure 6: DBZA in Dichloromethane IR spectrum

Results show the main carbon-oxygen double bond peak at 1654 cm^{-1}, which corresponds to the ZE conformer (Venkateshwarlu and Subrahmanyam). The ZE peak, which dominates the ZZ shoulder peak, differs from the Venkateshwarlu and Subrahmanyam findings, where they hypothesized that their prominent ZZ peak was due to steric hindrance. The intensities as a whole were much lower than the Venkateshwarlu and Subrahmanyam experiment, yet the ratio of EE conformer was very comparable to the Venkateshwarlu and Subrahmanyam experiment. This low intensity points to a high ratio of solvent in the resultant DBZA in dichloromethane sample. A triplet carbon oxygen double bond value is visible, yet the

presence of more ZE than ZZ conformer distinguishes these results from Venkateshwarlu and Subrahmanyam's findings. A new DBZA in dichloromethane sample was prepared and scanned on the second machine.

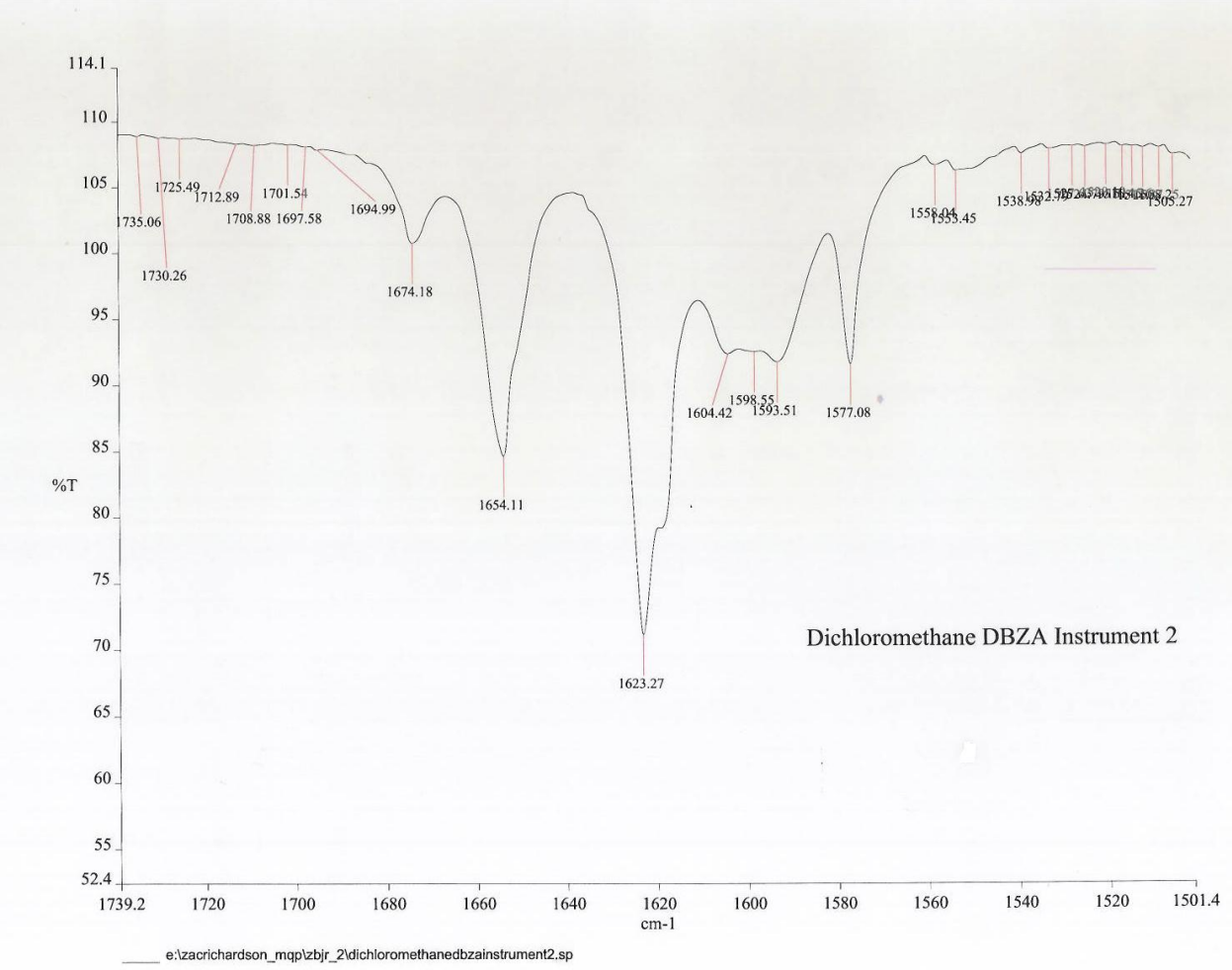

Figure 7: DBZA in Dichloromethane IR spectrum, take 2

The second time the results from the first instrument repeated themselves, only the intensities decreased, as the percent transmittance rose five percent. The presence of the same triplet peaks and the same relative intensities indicates the results are reproducible. The first IR graph was compared with predicted intensities and frequencies from the optimized structures of the ZZ, EE, and ZE conformers in dichloromethane at the B3LYP/6-311+G(d,p) level of theory.

The computed frequency values had to be adjusted accounting for the scale factor of 0.9688, which was obtained by comparing the frequencies of B3LYP/6-311+G(d,p) calculations, to account for the difference between B3LYP/6-311+G(d,p) level of theoretical results and real world results. (Merrick et al, 2010). These adjusted frequencies are compared to the experimental percent transmission below.

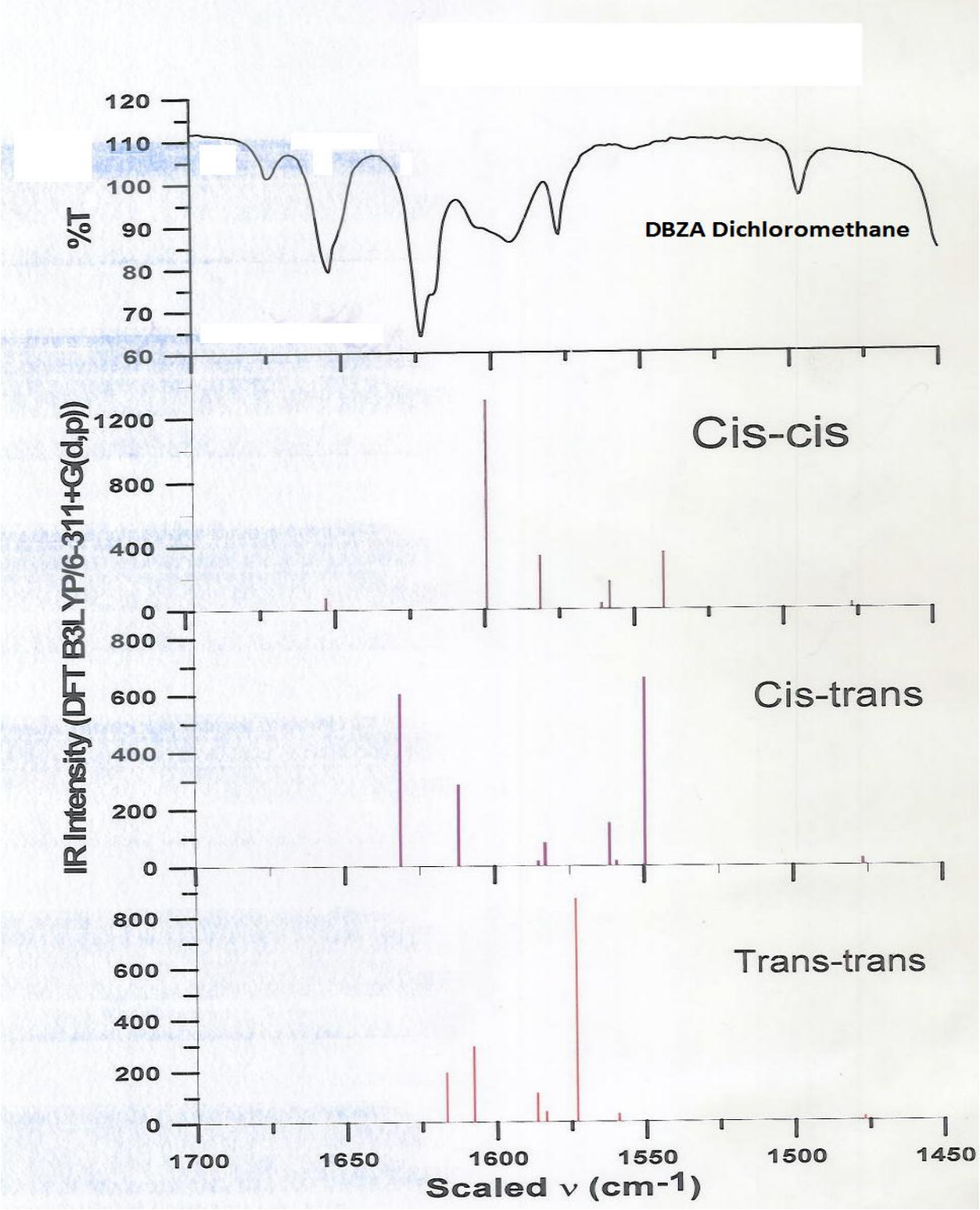

Figure 8: Second DBZA in Dichloromethane IR spectrum versus quantum molecular modeling predicted intensities and adjusted frequencies of DBZA in Dichloromethane

The strongly intense peaks from B3LYP/6-311+G(d,p) agree well to the intensities obtained experimentally. The ZE conformer's most intense peaks line up almost exactly with the most intense IR peak at about 1630 cm^{-1}. This correlates strongly with experimental data, showing the ZE conformer as being dominant in both mixtures of DBZA in dichloromethane. These findings are compared in Table 10.

EE adjusted frequency	EE Intensity	ZE adjusted frequency	ZE Intensity	ZZ adjusted frequency	ZZ intensity	Experimental frequency	Experimental intensity
1476.59	0.4595	1476.07	1.413	1476.37	0.3736	1476	105.708
1477.04	30.2759	1476.8	23.5827	1476.82	16.0058	1476.5	105.695
1540.18	355.588	1549.78	656.186	1559.31	29.5441	1477	105.701
1558.28	172.742	1559.34	16.075	1559.9	0.5349	1540	108.902
1560.93	36.1275	1561.65	149.315	1573.2	870.819	1550	107.407
1581.54	337.799	1583.2	79.6856	1583.65	39.3844	1558.5	108.136
1585.36	4.871	1585.51	16.2508	1586.6	110.748	1559.5	108.345
1599.39	1303.21	1612.1	284.49	1607.72	292.737	1560	108.208
1653.13	77.5487	1631.53	601.864	1616.9	192.558	1561	107.983
/	/	/	/	/	/	1561.5	108.04
						1573	100.722
						1581.5	99.8665
						1583	99.1668
						1583.5	98.6327
						1585	96.7044
						1585.5	95.9315
						1586.5	94.3062
						1599.5	88.3792
						1607.5	92.8566
						1612	95.7381
						1617	81.3607
						1631.5	102.191
						1653	82.5564

Table 10: DBZA computer predicted versus experimental intensities

The values computed by quantum molecular modeling and adjusted to scale may not be a perfect fit, yet they do show a ratio of ZE>ZZ>EE in dichloromethane based on closeness of the highest intensity peaks to the lowest percent transmittance regions of the IR spectrum.

The next most polar solvent was chloroform ($CHCl_3$). The actual IR spectrums of DBZA in chloroform were taken with the same procedure used for DBZA in dichloromethane.

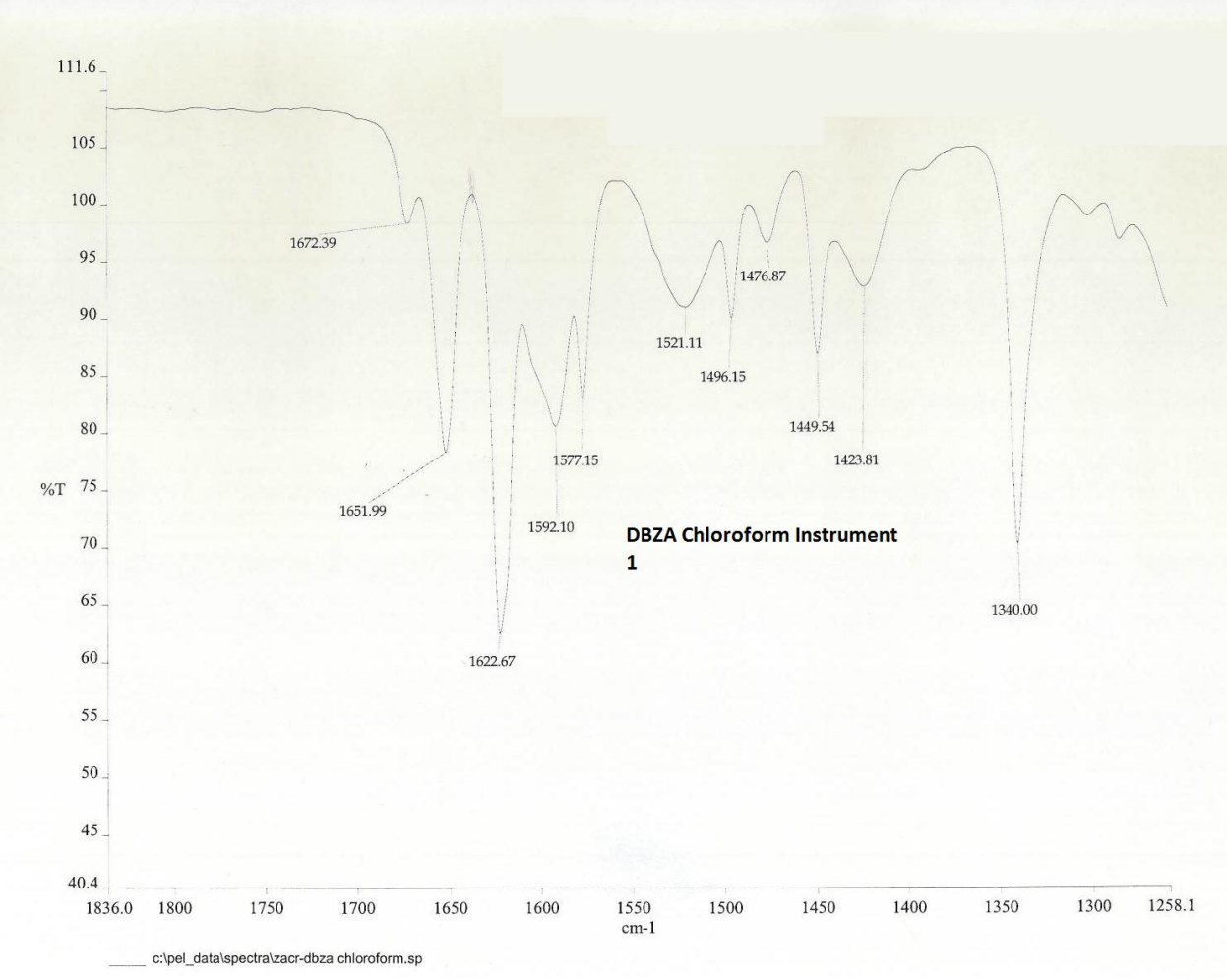

Figure 9: DBZA in chloroform IR spectrum

Here, the largest carbon-oxygen double bond peak lies at 1652 cm^{-1}, which is between the ZE and the ZZ values, and is closer to the ZE. The triplet peak just below 1650 cm^{-1} exists in roughly the same ratios to the ZE and EE peak intensities as in the first DBZA in dichloromethane spectra. The ZZ shoulder peak's relative intensity is much lower than in Venkateshwarlu and Subrahmanyam's findings.

This experiment was done again on a second machine with a new mixture of DBZA in chloroform.

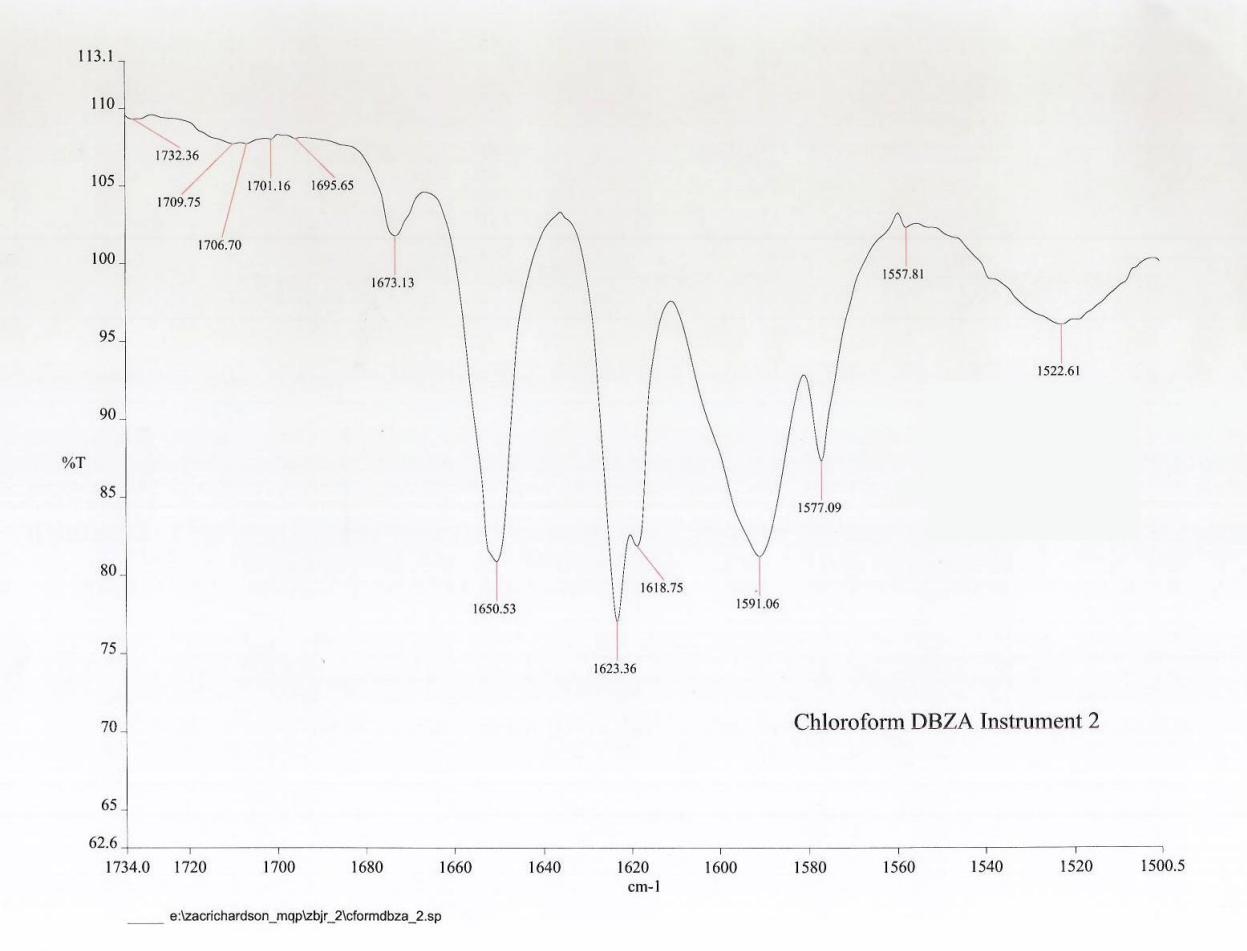

Figure 10: DBZA in chloroform IR spectrum take 2

Here, with the most intense carbon-oxygen double bond region peak measured at 1650.5 cm^{-1}, the spectrum shows that peak has a distinct shoulder with a slightly higher frequency. Even the carbon-carbon double bonding region shows a distinct shoulder peak. Only the intensity and frequency of the EE peak remains the same as in the first experiment. Here, the frequency of the 1650.5 cm^{-1} peak is slightly higher than its counterpart whose frequency matches the ZE region of Venkateshwarlu and Subrahmanyam's graph. Compared to

the corresponding Venkateshwarlu and Subrahmanyam experiment, the shape of the 1645-1655 cm^{-1} peak is exactly the same, if not for the fact that Venkateshwarlu and Subrahmanyam found the ZE conformer to be slightly more frequent than the ZZ, based on the intensities of their IR spectrum.

The second experiment correlates more strongly to the researched values (Venkateshwarlu and Subrahmanyam). Thus, the experimental IR spectrum from the second machine was compared to the intensities and adjusted frequencies obtained through quantum molecular modeling of all three conformers' for optimized geometries and vibrational frequencies in chloroform.

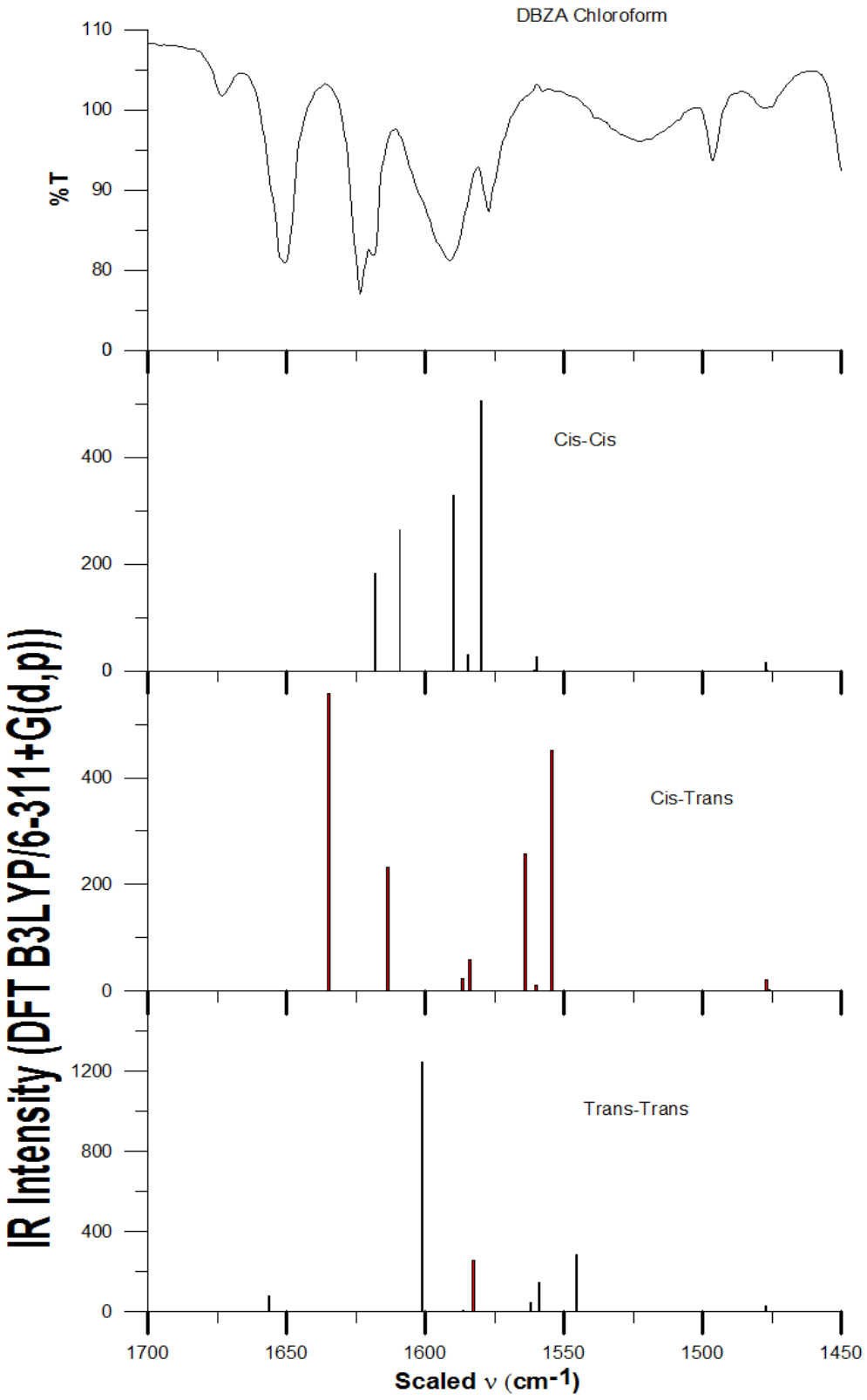

Figure 11: Second DBZA in Chloroform IR spectrum versus quantum molecular modeling predicted intensities and adjusted frequencies of DBZA in Chloroform

All three conformers have highly intense peaks which correlate somewhat to the IR spectrum, with the ZZ isomer making a direct connection at 1601 cm^{-1}. The ZE isomer has high intensity peaks very close to high intensity regions of the IR spectrum. This correlates to results showing ZZ>ZE>EE.

Table 11 directly compares the experimental and computational values. This is to show the values as plain numbers rather than merely interpret them from a graph.

EE adjusted frequency	EE Intensity	ZE adjusted frequency	ZE Intensity	ZZ adjusted frequency	ZZ intensity	Experimental frequency	Experimental intensity
1476.658	0.7124	1476.108	3.1595	1476.843	0.5509	1476	56.1481
1477.054	15.5764	1477.018	21.7234	1477.275	30.0434	1476.5	55.9783
1559.987	25.7779	1554.51	451.198	1545.656	283.078	1477	55.8602
1560.644	0.8845	1560.03	11.9943	1559.011	147.593	1477.5	55.8616
1579.788	505.366	1563.918	256.524	1561.971	48.2113	1545.5	65.4562
1584.451	30.1567	1584.007	60.2403	1582.64	255.02	1554.5	68.5175
1589.78	328.02	1586.485	24.5808	1586.22	5.7957	1560	68.2979
1609.142	263.613	1613.612	233.119	1601.169	1244.7	1560.5	67.7833
1618.16	182.299	1634.976	558.016	1656.377	76.0582	1562	66.6336
/	/	/	/	/	/	1564	65.1938
						1580	35.4133
						1582.5	40.042
						1584	37.3229
						1584.5	36.2292
						1586	33.0969
						1586.5	32.1158
						1590	26.8202
						1601	30.3434
						1609	36.1171
						1613.5	32.5314
						1618	12.4494
						1635	57.9105
						1656	25.1705

Table 11: DBZA computer predicted versus experimental intensities

These values, though not perfect, show that the ZE and ZZ isomers are much more present than the EE. Also, the ZZ peaks still fit the experimental results more closely than the ZE peaks.

Carbon tetrachloride is the last and least polar solvent studied. The experiment was done again in carbon tetrachloride.

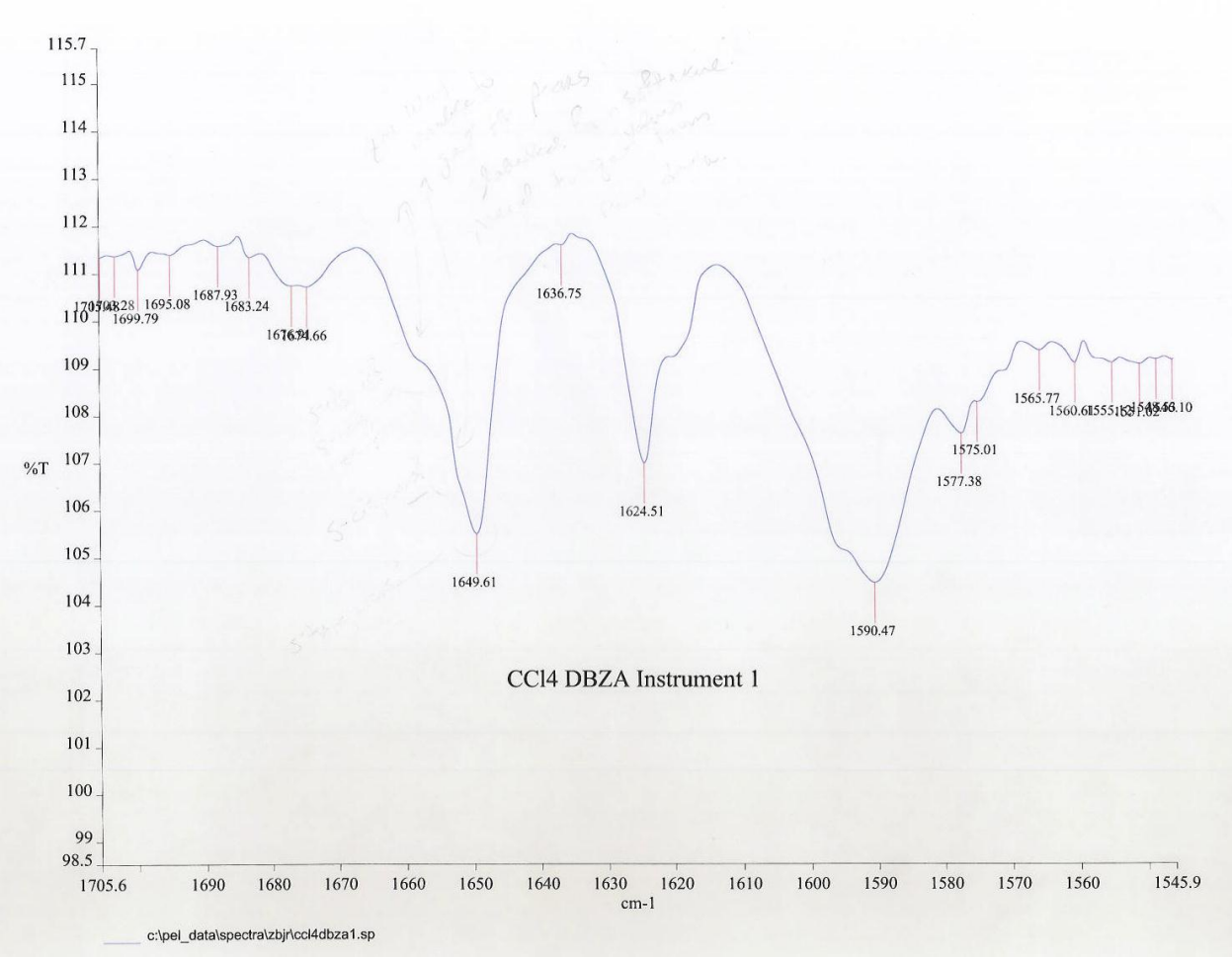

Figure 12: DBZA in CCl_4 Spectra machine 1

The main carbon-oxygen double bond region peak is at 1649.61 cm^{-1}. This value continues a trend of differing from Venkateshwarlu and Subrahmanyam's results, where the

main peak stood at 1654 cm^{-1}, which was in the ZE region. This experimental peak corresponds to the ZZ conformer region, which Venkateshwarlu and Subrahmanyam believed was sterically hindered in non polar solvent. The intensities of these peaks are very low compared to the dichloromethane and chloroform spectra, with the exception of the EE peak. This correlates to the Venkateshwarlu and Subrahmanyam findings, where the carbon tetrachloride intensities were lower in general, and the relative intensity of the EE peak is higher than in the first two solvents.

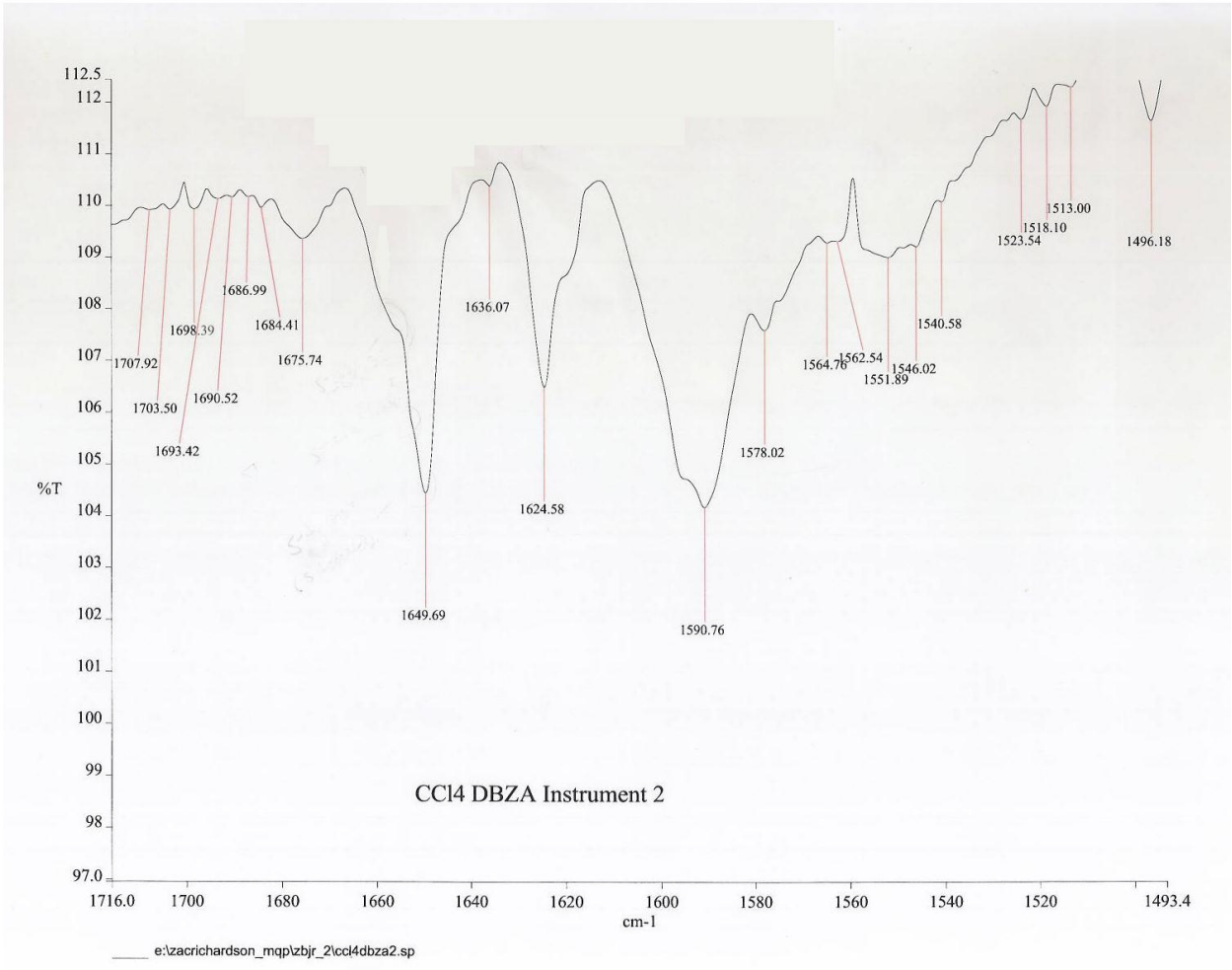

Figure 13: DBZA in CCl_4 Spectra machine 2

Once again, results are exactly the same, proving the experiment is reproducible. The first experiment had higher intensities, so it was compared to theoretical values.

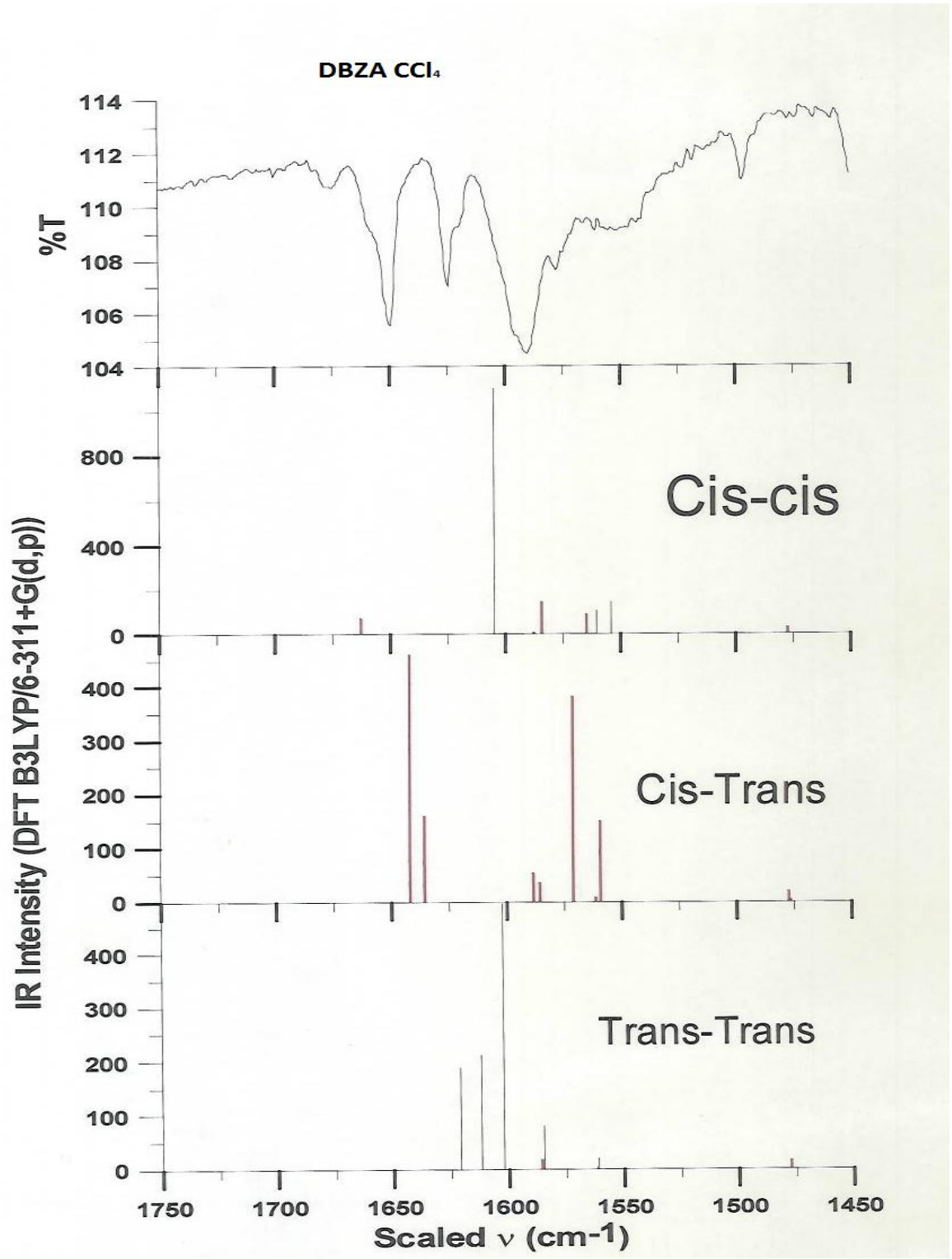

Figure 14: Second DBZA in carbon tetrachloride IR spectrum versus quantum molecular modeling predicted intensities and adjusted frequencies of DBZA in carbon tetrachloride

These values can be compared by this chart:

EE adjusted frequency	EE Intensity	ZE adjusted frequency	ZE Intensity	ZZ adjusted frequency	ZZ intensity	Experimental frequency	Experimental intensity
1477.224	0.6203	1476.701	2.9888	1477.179	1.3024	1477	113.193
1477.617	28.656	1477.49	20.6479	1477.501	14.6142	1477.5	113.264
1554.071	144.4809	1559.071	151.1111	1561.175	19.7868	1554	109.204
1560.285	109.7921	1561.26	8.7923	1561.852	3.3425	1559	109.517
1564.758	90.7859	1570.882	382.2339	1584.821	79.2567	1560.5	109.115
1584.397	144.4157	1585.482	35.0111	1585.82	17.389	1561	109.149
1587.826	8.3181	1588.523	53.3306	1602.128	495.6564	1561.5	109.264
1604.686	1099.499	1635.746	159.8334	1611.726	211.5233	1562	109.371
1662.783	72.562	1641.809	460.6063	1620.65	187.9745	1564.5	109.504
/	/	/	/	/	/	1571	108.938
						1584.5	106.961
						1585	106.701
						1585.5	106.412
						1586	106.113
						1588	105.07
						1588.5	104.855
						1602	107.847
						1604.5	108.73
						1611.5	110.976
						1620.5	109.236
						1635.5	111.815
						1642	111.028
						1663	110.837

Table 12: DBZA computer predicted versus experimental intensities

Values in all six experiments showed that the EE conformer is sterically hindered by chlorine rich solvents. The exact proportions of ZZ and ZE conformers and which one dominates depend on the mass of the solvent, rather than solely on its polarity.

UV-Vis Absorbance Studies of DBZA

The UV-Vis absorbance characteristics of DBZA were studied next. Using time-dependent density functional theory (TD-DFT), the absorbance characteristics and energies of each molecular orbital and energy state were calculated. The highest occupied molecular

orbital (HOMO), is shown for the highest bonding and non-bonding orbitals below for the EE isomer, as well as the lowest unoccupied molecular orbital (LUMO). These orbital shapes are shown below for the EE isomer.

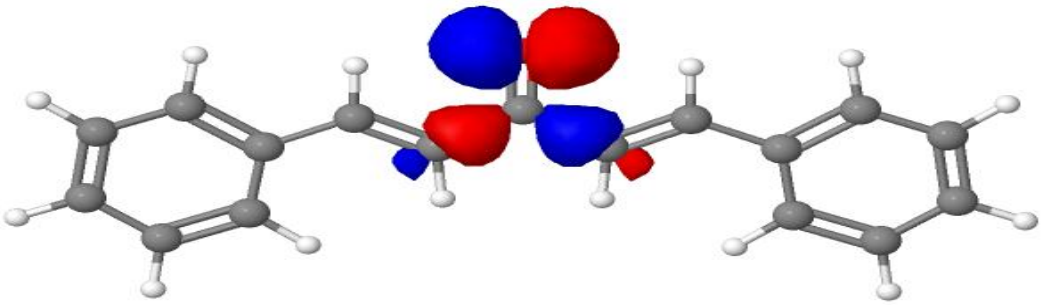

HOMO-2 (n)

MO 60

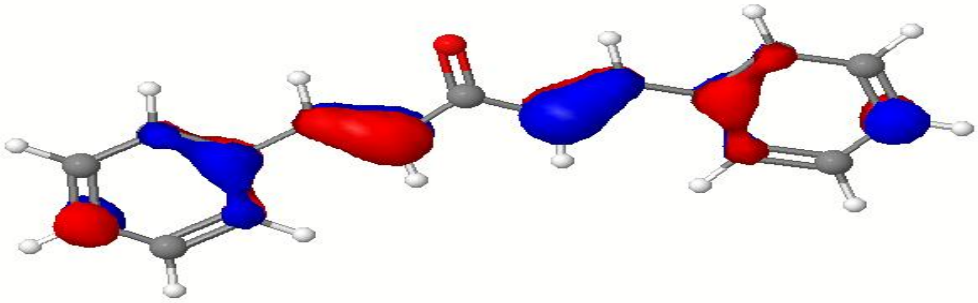

HOMO (π)

MO 62

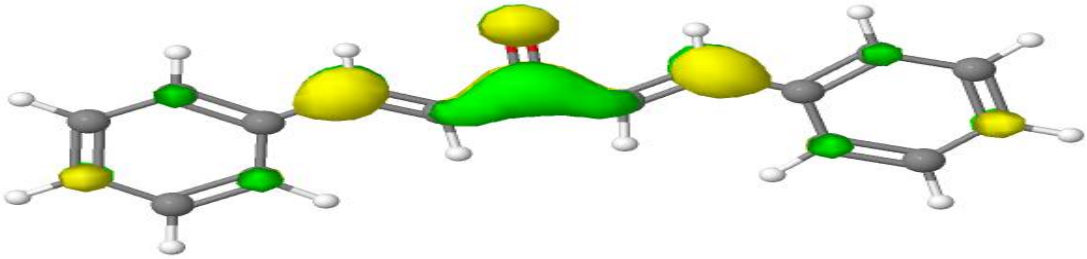

LUMO (π^*)

MO 63

Figure 15: EE conformer molecular orbitals

For the ZE conformer, the LUMO, HOMO and HOMO-2 orbitals can be seen below.

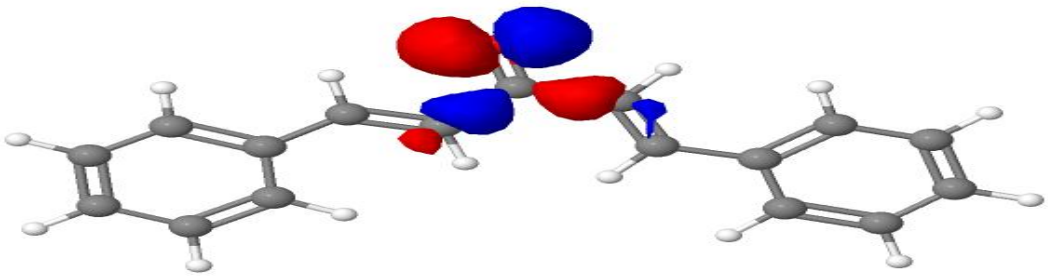

HOMO-2 (n)

MO 60

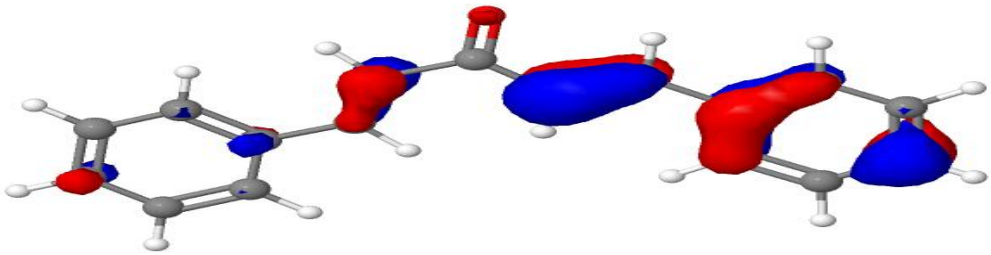

HOMO (π)

MO 62

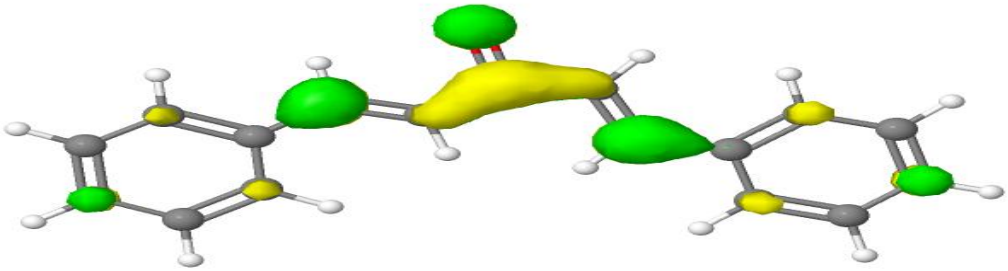

LUMO (π^*)

MO 63

Figure 16: ZE conformer molecular orbitals

As for the ZZ conformer, the HOMO, LUMO and HOMO-2 are also shown below.

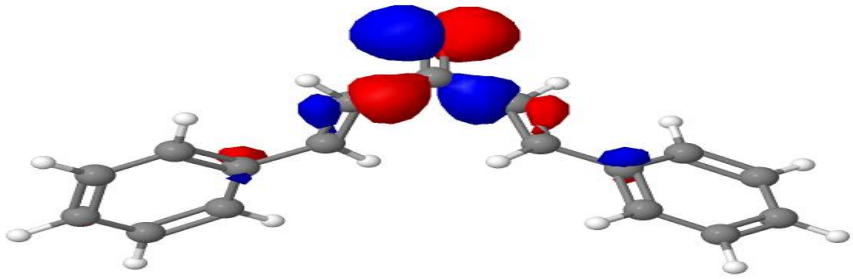

HOMO-2 (n)

MO 60

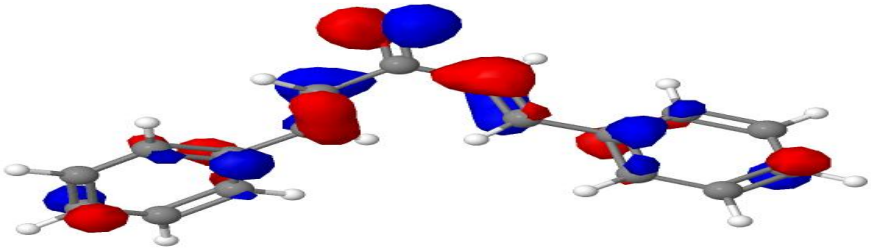

HOMO (π)

MO 62

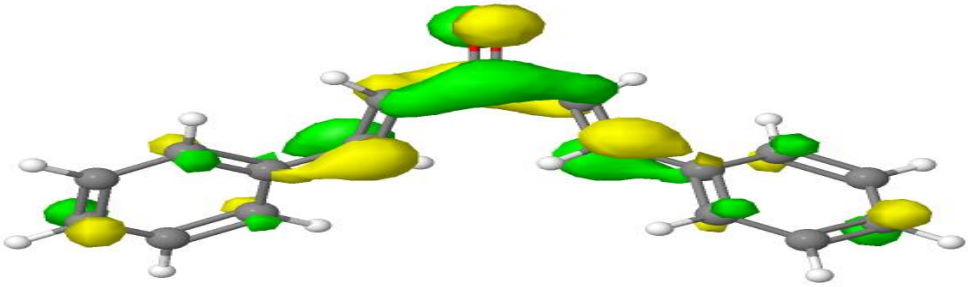

LUMO (π*)

MO 63

Figure 17: ZZ conformer Molecular orbitals

For all three conformers, the LUMO is molecular orbital number 63 and the HOMO for bonding and nonbonding orbitals are molecular orbitals 62 and 60, respectively. In all three cases, the LUMO is a $\pi*$ antibonding orbital, molecular orbital 62 is π bonding, and molecular orbital 60 is a nonbonding orbital localized on the carbonyl oxygen atom. With these same calculations, done at the DFT B3LYP/6-311+G(d,p) level of theory, the actual molecular orbital data could be found. This entailed the transition energies, oscillator strengths, and wavelengths for each state, as well as the configuration interaction coefficients for each molecular orbital transition at that level. The computed values at this level of theory are presented in Table 13.

Isomer	State	Transition energy (eV)	Transition frequency (cm^{-1})	Transition λ (nm)	Oscillator strength	MO	CI Coefficient
ZZ	S_1 (n,π*)	3.4813	28090	356.14	0.0054	60 -> 63 60 -> 68 62 -> 63	0.57514 0.11138 -0.38152
	S_2 (π,π*)	3.9787	32051	311.62	0.4374	61 -> 63	0.69685
	S_3 (π,π*)	4.1021	33113	302.24	0.0913	60 -> 63 61 -> 64 62 -> 63	0.36946 0.25672 0.54029
	S_4 (π,π*)	4.1518	33445	298.63	0.1449	60 -> 64 62 -> 64	-0.35867 0.59198
	S_5 (π,π*)	4.2118	34014	294.38	0.0146	58 -> 64 59 -> 63 61 -> 65 62 -> 66	-0.14812 0.63838 -0.18515 -0.16611
ZE	S_1 (n,π*)	3.1125	25104	398.34	0	60 -> 63 60 -> 68	0.69692 -0.10622
	S_2 (π,π*)	3.5551	28673	348.75	0.7231	62 -> 63	0.70244
	S_3 (π,π*)	3.8426	30992	322.66	0.1643	61 -> 63 62 -> 64	0.67022 0.20318
	S_4 (π,π*)	3.9669	31995	312.54	0.0069	59 -> 63 62 -> 66	0.67367 -0.16880
	S_5 (π,π*)	3.9698	32018	312.32	0.0113	58 -> 63 61 -> 65 62 -> 65	0.66682 -0.16744 -0.12008
EE	S_1 (n,π*)	2.9862	24085	415.19	0	60 -> 63	0.69881
	S_2 (π,π*)	3.4701	27988	357.29	1.0612	62 -> 63	0.70603
	S_3 (π,π*)	3.7625	30346	329.53	0.0393	61 -> 63 62 -> 64	0.68907 -0.14523
	S_4 (π,π*)	3.7645	30362	329.35	0.0109	59 -> 63 61 -> 66 62 -> 65	0.68211 0.10522 0.13032
	S_5 (π,π*)	3.929	31689	315.57	0.0068	58 -> 63 61 -> 65 62 -> 66	0.68058 0.10887 0.13086

Table 13: Molecular energies of all three conformers

Molecular orbital calculations were done for each conformer in n-hexane, which was used in the experiment by Hoshi et al. First, the computed values at the TD-DFT B3LYP/6-311+G(d,p) level of theory are listed below for these results.

Isomer	State	Transition energy (eV)	Transition frequency (cm^{-1})	Transition λ (nm)	Oscillator strength	MO	CI Coefficient
ZZ	S_1 (n,π*)	3.3848	27300	366.3	0.0099	60 -> 63 60 -> 67 61 -> 63	0.6074 0.1122 0.331
	S_2 (π,π*)	3.6651	29560	338.29	0.5862	62 -> 63	0.703
	S_3 (π,π*)	3.9167	31591	316.55	0.1528	60 -> 63 61 -> 63 62 -> 64	-0.3277 0.5858 -0.2116
	S_4 (π,π*)	3.9706	32025	312.26	0.0288	58 -> 63 59 -> 64 61 -> 64 62 -> 65 62 -> 66	0.6296 0.1195 -0.2094 0.1289 0.1487
	S_5 (π,π*)	3.9746	32057	311.94	0.0209	58 -> 64 59 -> 63 61 -> 66 62 -> 65	0.1236 0.663 0.1343 0.1528
ZE	S_1 (n,π*)	3.1907	25735	388.58	0	60 -> 63 60 -> 68	0.6973 -0.1037
	S_2 (π,π*)	3.4465	27798	359.74	0.8893	62 -> 63	0.7044
	S_3 (π,π*)	3.7970	30625	326.53	0.1851	61 -> 63 62 -> 64	0.6854 0.1558
	S_4 (π,π*)	3.892	31390	318.57	0.0097	59 -> 63 62 -> 66	0.68032 -0.144
	S_5 (π,π*)	3.9584	31926	313.22	0.0161	58 -> 63 61 -> 65 62 -> 65	0.6763 -0.1368 -0.1116
EE	S_1 (n,π*)	3.0543	24634	405.94	0	60 -> 63	0.69906
	S_2 (π,π*)	3.3425	26959	370.93	1.2171	62 -> 63	0.70605
	S_3 (π,π*)	3. 6935	29790	335.68	0.0537	61 -> 63 62 -> 64	0.6967 -0.1058
	S_4 (π,π*)	3.7355	30129	331.91	0.0135	59 -> 63 62 -> 65	0.68725 0.11441
	S_5 (π,π*)	3.9282	31684	315.62	0.0103	58 -> 63 62 -> 66	0.68587 0.11511

Table 14: Molecular energies of all three conformers

The DBZA in n-hexane absorption spectra experiment had to be done twice. First, absorbance was run in order to observe $\pi* \leftarrow$ n absorbance at around 360 nm (Hoshi et al). Next, DBZA was diluted thirty-fold from stock concentrated solution in experiment one in order to recognizably view the $S_2(\pi, \pi^*)$ absorbance band.

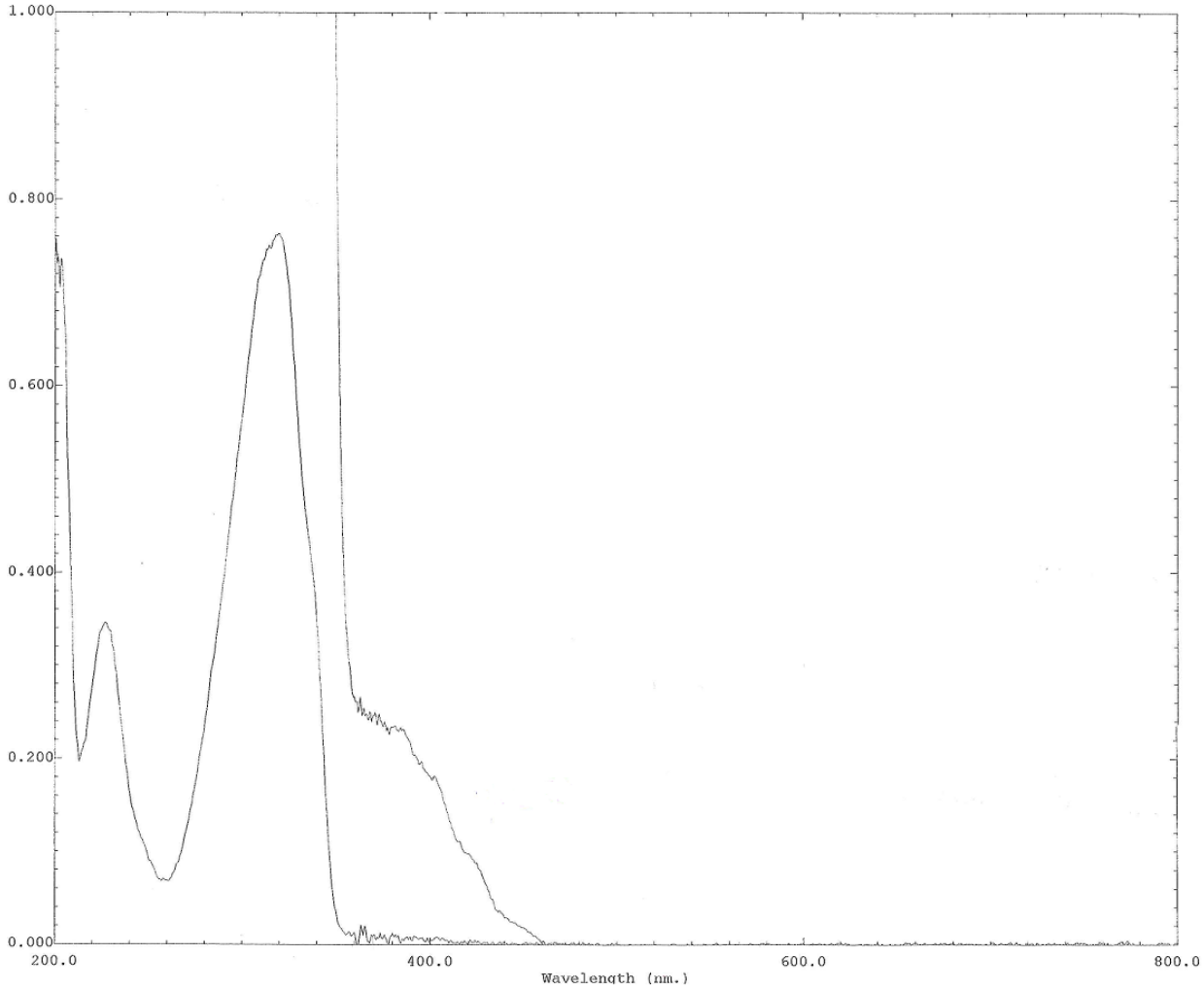

Figure 18: Experimental UV-visible spectra of DBZA and 30 times diluted DBZA in n-Hexane

These results match the Hoshi et al results perfectly in terms of peak shapes and frequencies except the peak of the third transition state is just slightly skewed right. The intensity values are twice as high as those obtained by Hoshi et al in both experiments, which

once again indicates a difference in concentration of solute versus solvent. Comparing these results to those obtained theoretically gives a different picture.

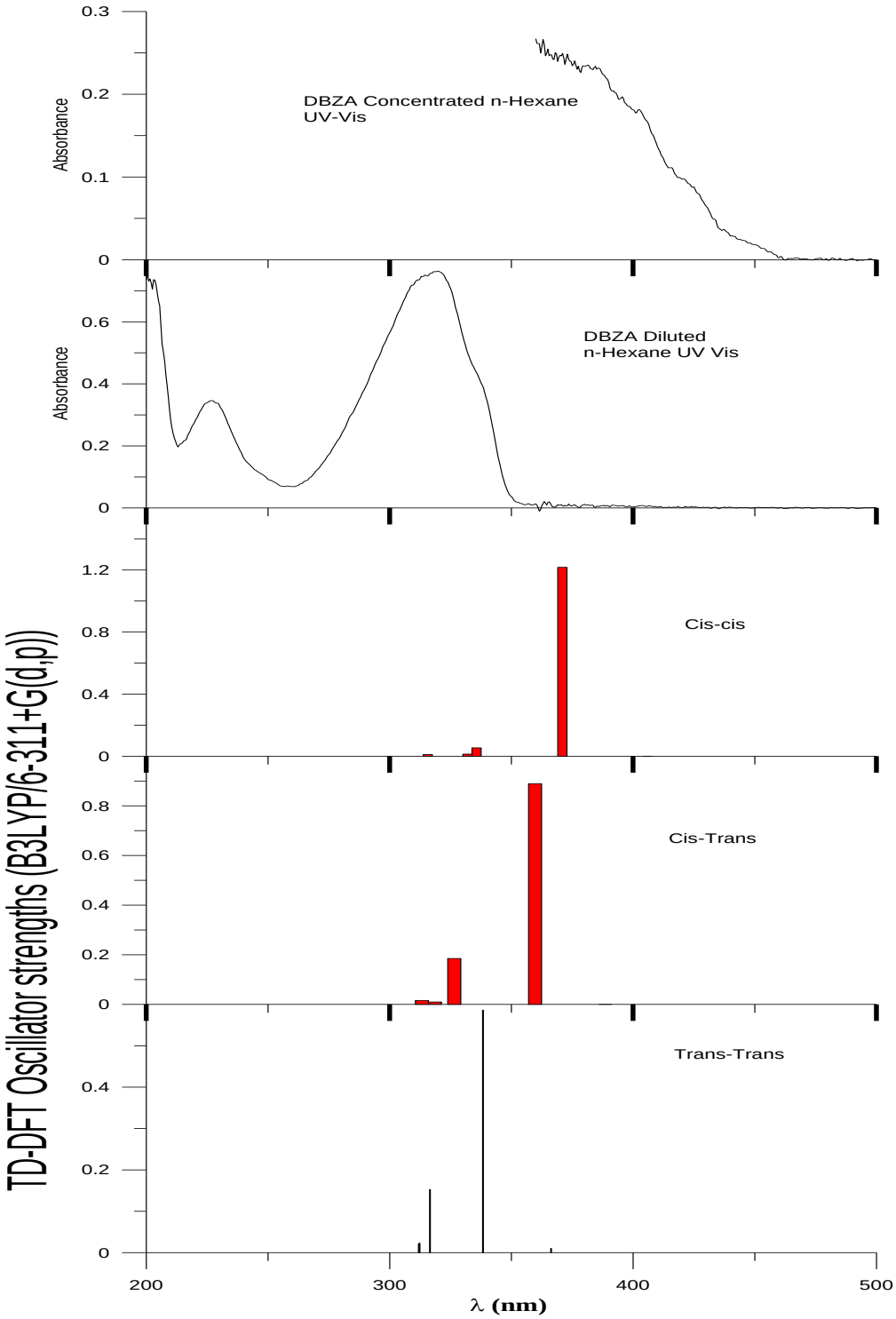

Figure 19: Grapher comparison of wavelength versus absorbance for experimental and computed DBZA in n-Hexane UV-visible spectra

The graph shows the presence of all three conformers. The EE conformer has its strongest peak in a lower absorbance section of the spectra than the ZZ and ZE conformers do, but not by very much. This shows that even in non halogenated solvents, the EE conformer is at least somewhat sterically hindered. To compare these values further, they are presented in the table below.

EE λ (nm)	Oscillator strength	ZE λ (nm)	Oscillator strength	ZZ λ (nm)	Oscillator strength	Experimental λ (Concentrated) (nm)	Experimental Absorbance (Concentrated)
406	0	389	0	366	0.0099	405	0.1696
371	1.2171	360	0.8893	338	0.5862	388.5	0.2210
336	0.0537	327	0.1851	317	0.1528	371	0.2495
332	0.0135	319	0.0097	312	0.0228	366.5	0.2475
316	0.0103	313	0.0161	312	0.0209	360	0.2671
						Experimental λ (dilute) (nm)	Absorbance (dilute)
						359.5	0.0120
						338.5	0.3873
						335.5	0.4383
						332	0.4997
						326.5	0.6663
						318.5	0.7617
						316.5	0.7554
						315.5	0.7474
						313	0.7467
						312.5	0.7400
						312	0.7345

Table 15: Comparison of quantum molecular modeling absorbance versus experimental absorbance

Values may not be a perfect fit, but they still show all three isomers are present. The experiment was performed again in chloroform. The theoretical values are as follows.

Isomer	State	Transition energy (eV)	Transition frequency (cm^{-1})	Transition λ (nm)	Oscillator strength	MO	CI Coefficient
ZZ	S_1 (n,π*)	3.6317	29292	341.39	0.0129	60 -> 63 60 -> 67 61 -> 63	0.60962 0.11346 0.31643
	S_2 (π,π*)	3.8446	31009	322.49	0.5934	62 -> 63	0.70337
	S_3 (π,π*)	4.0396	32582	306.92	0.1603	60 -> 63 61 -> 63 62 -> 64	-0.31674 0.60141 0.18234
	S_4 (π,π*)	4.1263	33281	300.47	0.0104	58 -> 64 59 -> 63 61 -> 65 62 -> 66	0.1273 0.6577 -0.1315 0.1474
	S_5 (π,π*)	4.1307	33316	300.16	0.0235	58 -> 63 59 -> 64 61 -> 66 62 -> 65	0.6594 0.1231 -0.1345 0.1484
ZE	S_1 (n,π*)	3.2705	26378	379.1	0	60 -> 63 60 -> 67	0.6977 -0.10113
	S_2 (π,π*)	3.4033	27450	364.3	0.9354	62 -> 63	0.7052
	S_3 (π,π*)	3.7582	30311	329.91	0.1789	61 -> 63 62 -> 64	0.68817 0.14664
	S_4 (π,π*)	3.8633	31159	320.93	0.0101	59 -> 63 62 -> 66	0.6846 -0.12631
	S_5 (π,π*)	3.9548	32018	312.32	0.0177	58 -> 63 61 -> 65 62 -> 65	0.68199 0.1158 0.1043
EE	S_1 (n,π*)	3.1233	25191	396.97	0	60 -> 63	0.69935
	S_2 (π,π*)	3.2984	26604	375.89	1.2513	62 -> 63	0.70604
	S_3 (π,π*)	3.6728	29623	337.57	0.0578	61 -> 63	0.69752
	S_4 (π,π*)	3.7301	30085	332.39	0.0148	59 -> 63 62 -> 65	0.69037 0.10453
	S_5 (π,π*)	3.9325	31718	315.28	0.0108	58 -> 63 62 -> 66	0.68897 0.10548

Table 16: Molecular energies of all three conformers

The actual experiment involved dilute DBZA in chloroform. Here is the spectrum of results.

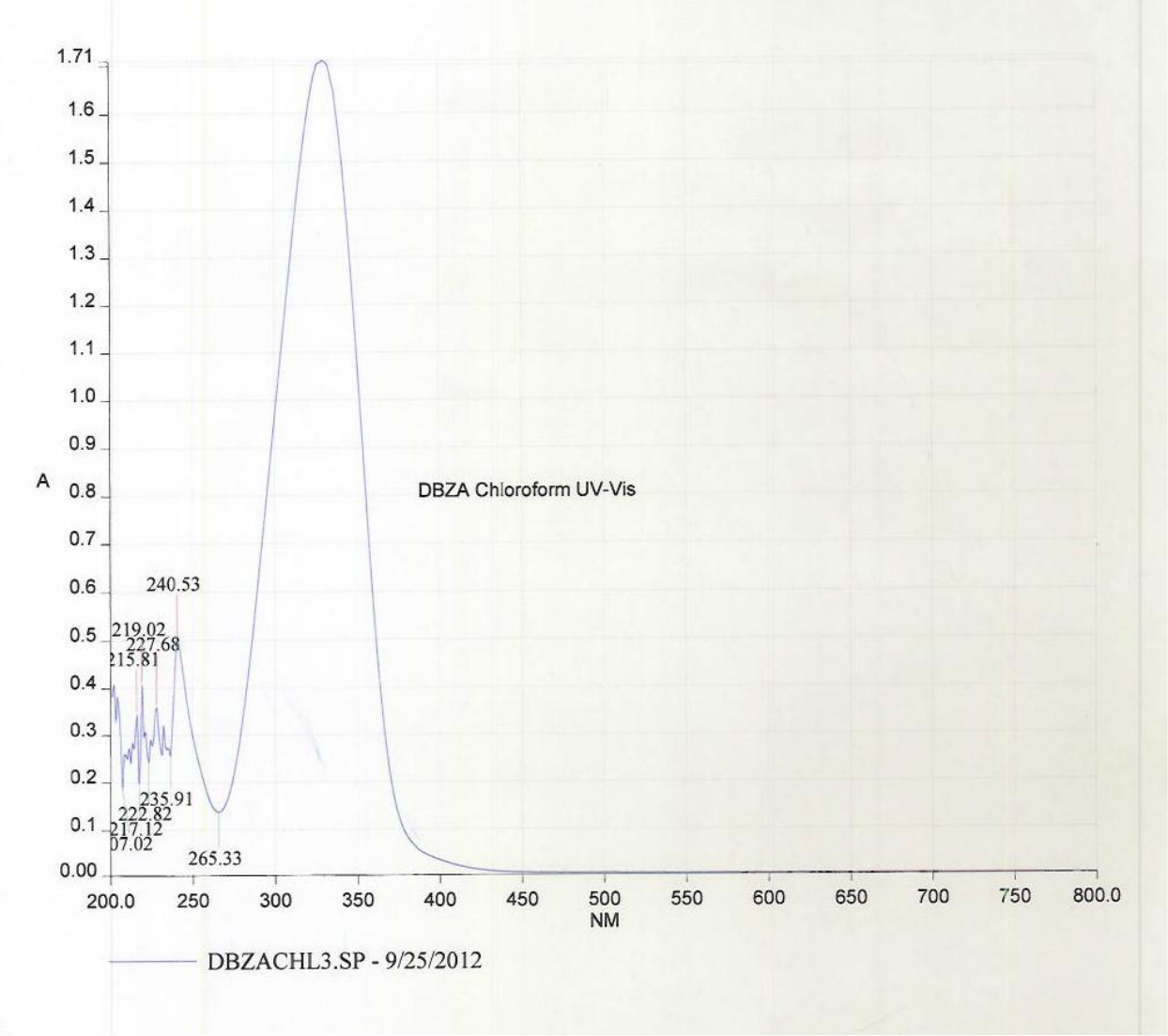

Figure 20: UV-Vis spectra of DBZA in Chloroform

The results show a much higher absorbance than in n-Hexane, so the n to π^* transition can be observed along with all the other transition states in one experiment. Molecular absorbance values from this experiment had to be compared to theoretical absorbance values and wavelengths.

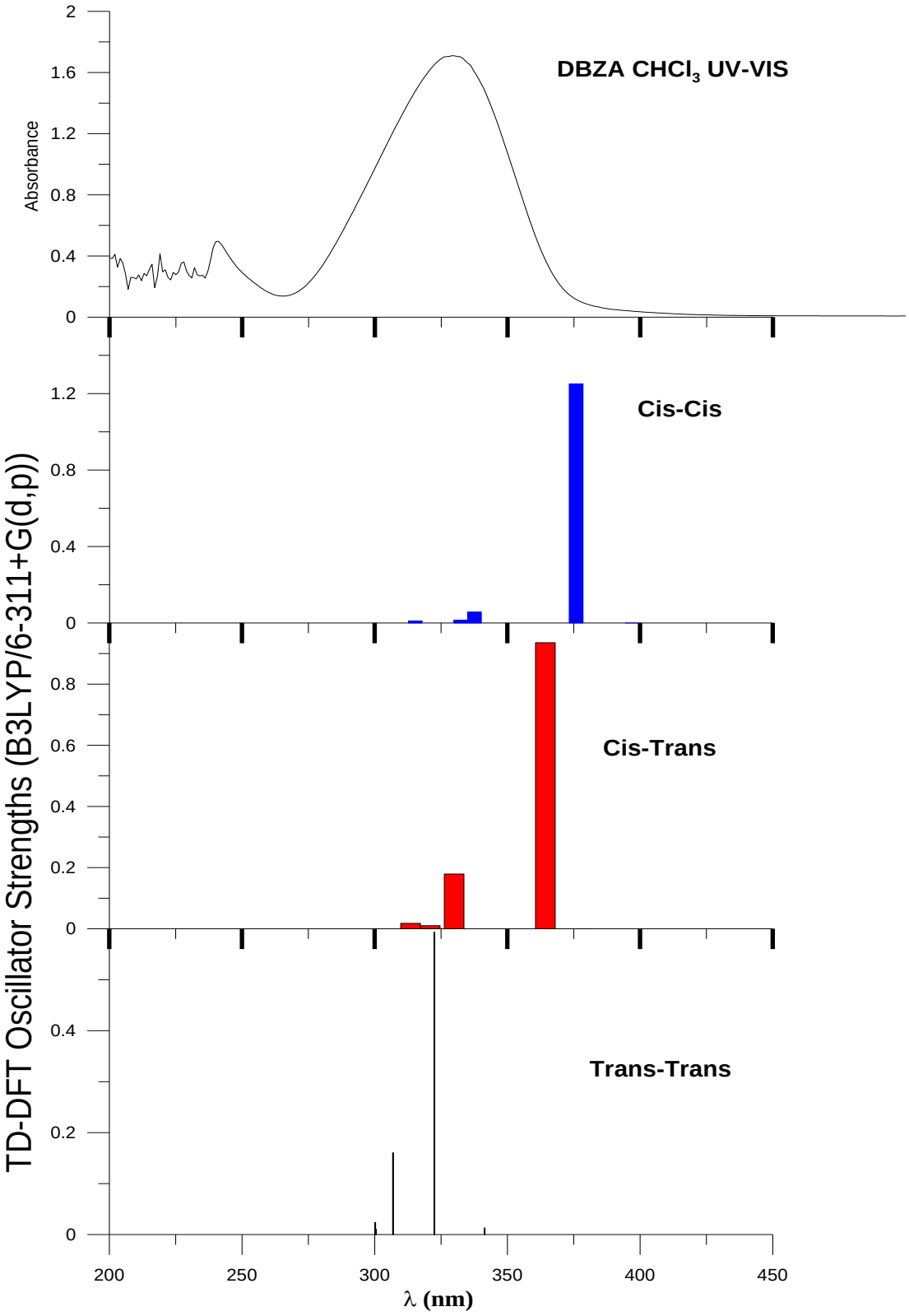

Figure 21: Grapher comparison of wavelength versus absorbance for experimental and computed DBZA in $CHCl_3$ UV-visible spectra

The ZZ conformer stands head and shoulders above the ZE and the EE conformers in terms of prevalence from the given experimental spectra. These values are compared in this table.

EE λ (nm)	Oscillator strength	ZE λ (nm)	Oscillator strength	ZZ λ (nm)	Oscillator strength	Experimental λ (nm)	Experimental Absorbance
397	0	379	0	341	0.0129	300	0.97411
376	1.2513	364	0.9354	322	0.5934	301	1.0085
338	0.0578	330	0.1789	307	0.1603	307	1.21712
332	0.0148	321	0.0101	300	0.0104	314	1.44145
315	0.0108	314	0.0177	300	0.0235	315	1.47318
						321	1.62387
						322	1.6433
						330	1.70878
						332	1.70335
						338	1.58998
						341	1.49546
						364	0.38175
						376	0.11386
						379	0.09059
						397	0.03903

Table 17: Comparison of quantum molecular modeling versus experimental absorbance of DBZA in chloroform

The computed values line up nicely with the experimental ones. The experiment was a success.

Conclusions

DBZA does indeed form three conformers under various conditions and in certain solvents. The proportions of these isomers vary when DBZA is dissolved in carbon tetrachloride, chloroform, and dichloromethane. The EE conformer may be the major form in the solid state of DBZA in air, but in all solvents tested, it is sterically hindered to the point of being the least prevalent of the three. Whether the ZE or skewed ZZ conformer comes to dominate depends on the size of solvent and concentration of the solute, and not just on solvent polarity.

Appendices

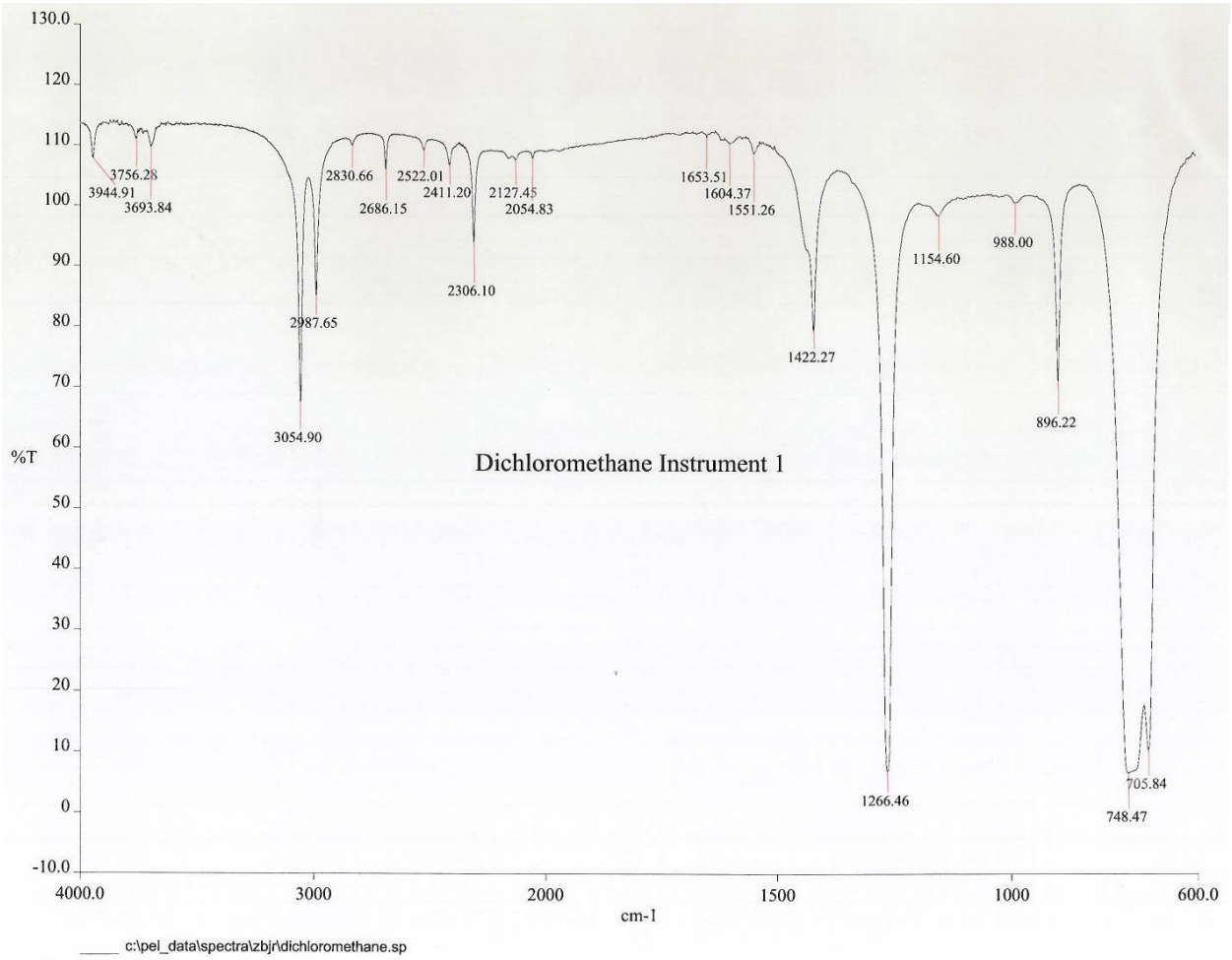

Figure 22: IR spectrum of Dichloromethane

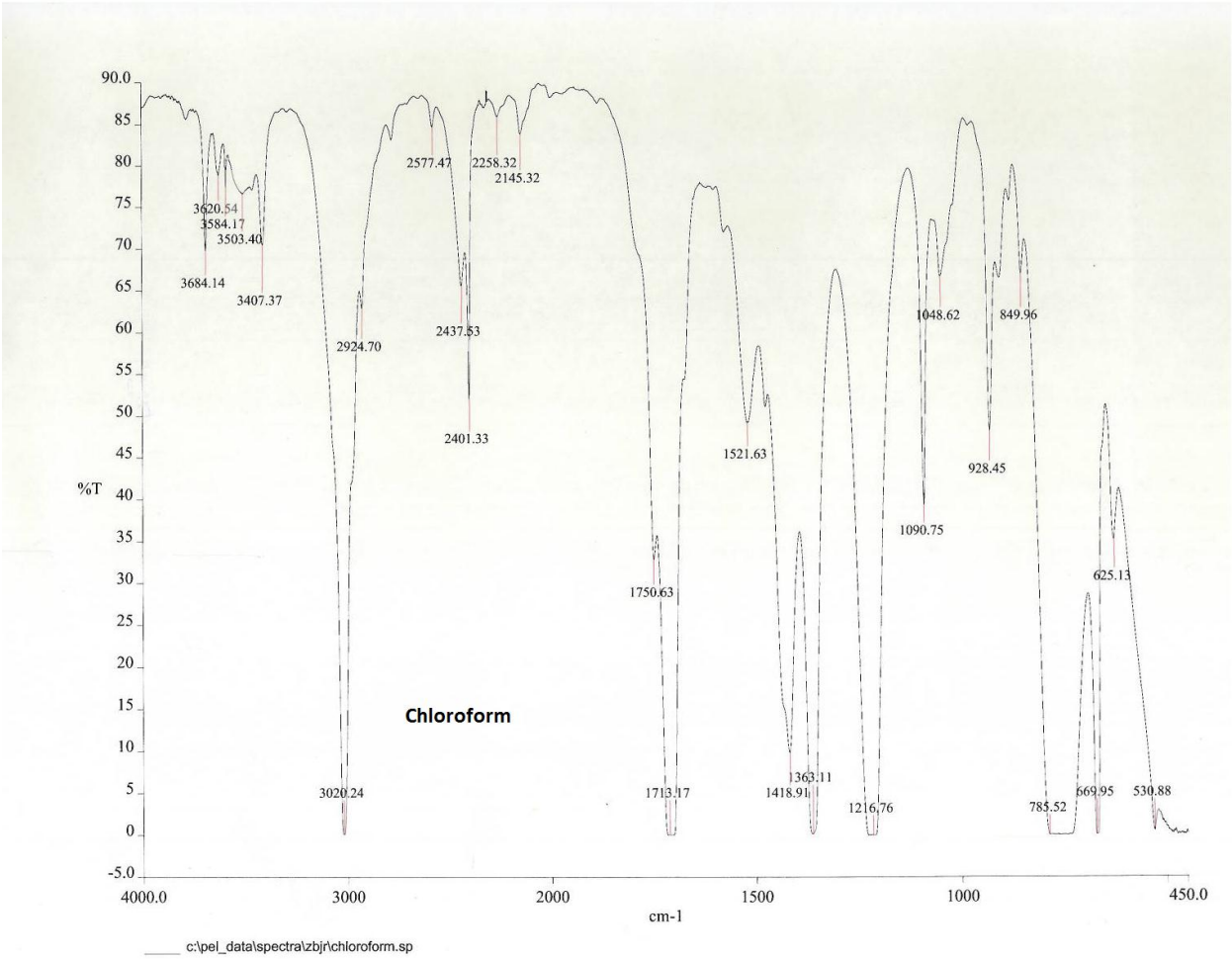

Figure 23: IR spectrum of Chloroform

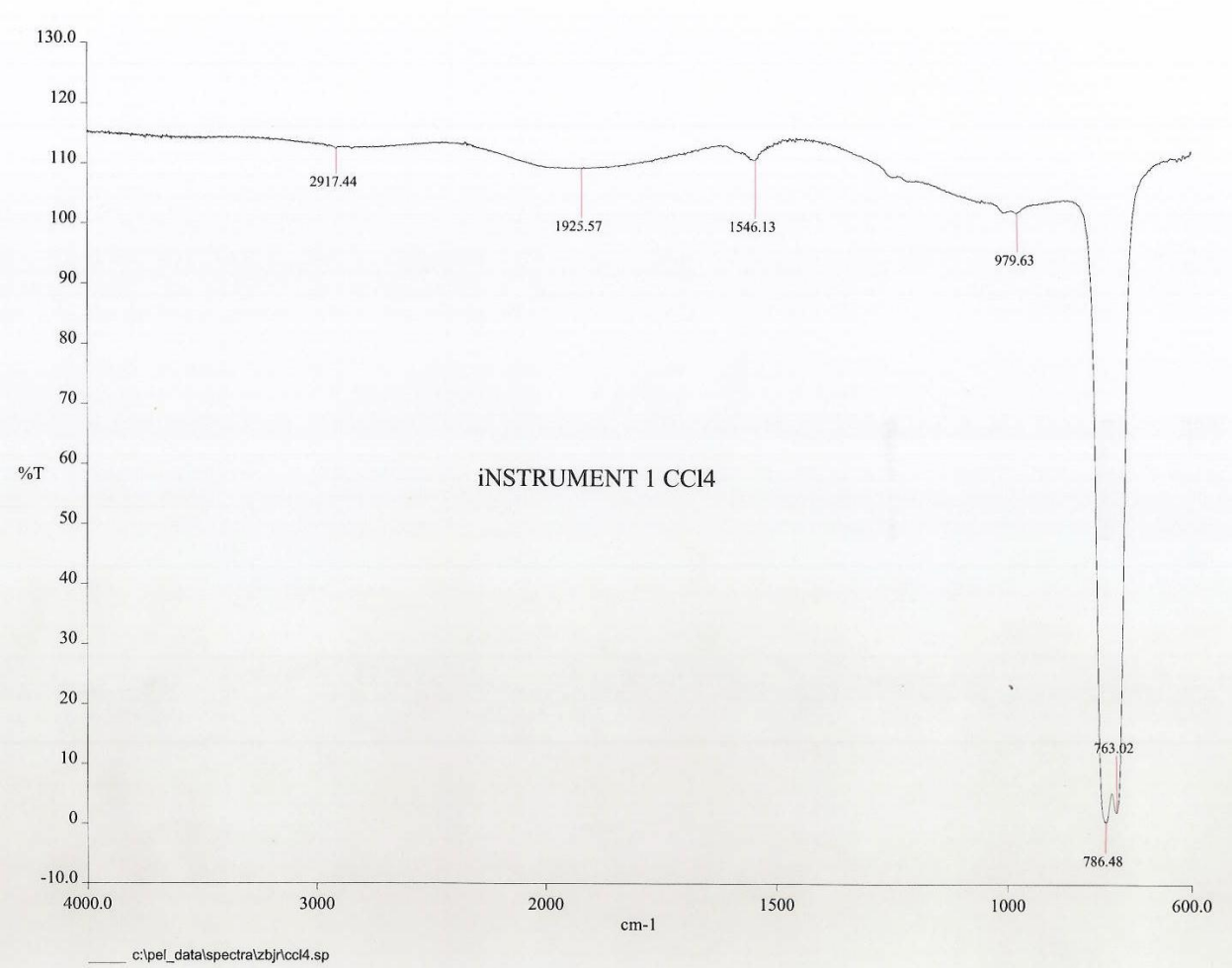

Figure 24: IR spectrum of Carbon Tetrachloride

References

Bhandarkar SS, Bromberg J, Carrillo C, Selvakumar P, Sharma RK, Perry BN, Govindarajan B, Fried L, Sohn A, Reddy K,Arbiser JL. “Tris (dibenzylideneacetone) dipalladium, an N-myristoyltransferase-1 inhibitor, is effective against melanoma growth in vitro and in vivo.” Department of Dermatology, Emory University School of Medicine, Atlanta, GA 30322, USA. 2008 Sep 15; http://www.ncbi.nlm.nih.gov/pubmed/18794083?dopt=AbstractPlus

Bramley R. and R. J. W. Le Fèvre. “Molecular polarisability: phenylpolyenals and diphenylpolyene ketones” J. Chem. Soc., 1962, 56-63 http://pubs.rsc.org/en/content/articlelanding/1962/jr/jr9620000056

T. Hoshi, T. Kawashima, J. Okubo, M. Yamamoto, H. Inoue, “Conformations and electronic structures of Dibenzylideneacetone,” J. Chem. Soc., Perkin Trans 2 (1986) 1147–1150. http://pubs.rsc.org/en/content/articlepdf/1986/p2/p29860001147

Huck, Lawrence A., and William J. Leigh. "A Better Sunscreen: Structural Effects on Spectral Properties." - Journal of Chemical Education (ACS Publications and Division of Chemical Education). Department of Chemistry and Chemical Biology, McMaster University, Hamilton ON, L8S 4M1, Canada, 6 Oct. 2010. Web. 08 Oct. 2012. <http://pubs.acs.org/doi/abs/10.1021/ed1004867>.

Merrick, Jeffrey P, Damian Moran, and Leo Radom. “An Evaluation of Harmonic Vibrational Frequency Scale Factors” School of Chemistry and Centre of Excellence in Free Radical Chemistry and Biotechnology, University of Sydney, Sydney, New South Wales 2006, Australia

J. Phys. Chem. A, 2007, 111 (45), pp 11683–11700 DOI: 10.1021/jp073974n

http://homepage.univie.ac.at/mario.barbatti/papers/method/vib_scale_factors_radom_2007.pdf

Shoppee, Charles W., Wang, Yueh-Sha, Sternhell, Sever, Brophy, Graham C. Electrocyclic reactions. Part X. Photochemical cyclization of *Trans, trans*-Dibenzylideneacetone. *J. Chem. Soc*., *Perkin Trans. 1*(1976), pp. 1880-1886.

Surov, S. V. Tsukerman, V. D. Orlov, Yu. N., and V. F. Lavrushin. "Dipole Moments of Dibenzylidenecycloalkanones and Some of Their Analogs." *SpringerLink*. Springer Science+Business Media, 17 Oct. 1966. Web. 08 Oct. 2012. <http://www.springerlink.com/content/p328p59wp3433414/>.

Tanaka, Hisao, Koh-ichi Yamada, and Hiroshi Kawazura. "The Conformations and 1H Nuclear Magnetic Resonance Parameters of Dibenzylideneacetone." *Journal of the Chemical Society, Perkin Transactions 2 (RSC Publishing)*. J. Chem. Soc., Perkin Trans. 2, 1978. Web. 08 Oct. 2012. <http://pubs.rsc.org/en/content/articlepdf/1978/p2/p29780000231>.

K. Vanchinathan, G.Bhagavannarayana, K.Muthu, S.P.Meenakshisundaram. “Synthesis, crystal growth and characterization of 1,5-diphenylpenta-1,4-dien-3-one: An organic crystal.” Department of Chemistry, Annamalai University, Annamalainagar 608 002, Chennai, India. 13 March 2011. www.elsevier.com/locate/physb

Vaucher, Alain. “Aldol condensation, recrystallization Synthesis of (E,E) – dibenzylideneacetone” Zurich, March 14, 2011. http://www.n.ethz.ch/~avaucher/download/reports/OACPI/Exp2.pdf

Venkateshwarlu, G., and B. Subrahmanyam. "Conformations of Dibenzylideneacetone: An IR Spectroscopic Study." *SpringerLink*. Springer Science Business Media, 9 Oct. 1987. Web. 08 Oct. 2012. <http://www.springerlink.com/content/n52340g7761335t1/>.